Supplementary Information

Design of activatable NIR-II molecular probe for in vivo elucidation of disease-related viscosity variations

Kun Dou [†], Weijing Huang[†], Yunhui Xiang[†], Songjiao Li[†], Zhihong Liu*[,†,‡]

[†]Key Laboratory of Analytical Chemistry for Biology and Medicine (Ministry of Education), College of Chemistry and Molecular Sciences, Wuhan University, Wuhan, Hubei 430072, China.

[‡]State Key Laboratory of Applied Organic Chemistry （Lanzhou University), Lanzhou 730000, China.

E-mail: zhhliu@whu.edu.cn

Tel: +86-27-87217886

Fax: +86-27-68754067

Table of Contents

Materials and apparatus

Unless otherwise stated, all reagents and materials were purchased from commercial accompany and used without further purification. IR-1061, Indocyanine Green (ICG), and Lipopolysaccharide (LPS) were purchased from Sigma-Aldrich. 3-(4,5-dimethylthiazol-2-yl)-2,5-diphenyltetrazolium bromide (MTT), 3-Ethyl-2,4-dimethylpyrrole, anhydrous dichloromethane and DMF were purchased from Aladdin Reagent Co., Ltd (Shanghai, China). Streptozotocin (STZ), Resveratrol (RVT), Monensin (Mon) and Nystatin (Nys) were purchased from Energy Chemical Co., Ltd (Shanghai, China). Acetonitrile (CH_3CN), Dimethyl sulfoxide (DMSO), N,N-Dimethylformamide (DMF), CH_3OH, Glycerol, Ethanol, Acetone, petroleum ether and ethyl acetate were analytical grade without further purification. Mass spectrometry was performed on Ultimate3000&Compact (Bruker, Germany), Scientific LTQ Orbitrap Elite (Thermo Fisher, America) mass spectrometers. The ^{1}H-NMR and ^{13}C-NMR spectra were acquired over a Bruker AV-400 spectrometer. Absorption spectra were recorded on a UV-vis-NIR spectrophotometer (Shimadzu UV-2550, Japan). NIR-II fluorescence spectra were excited by 808-nm laser (Beijing Hi-Tech Optoelectronic Co., Ltd.) and recorded with a fluorometer (Fluorolog-3, Horiba Jobin Yvon, France).

Synthesis and Characterization

Synthesis of phenyl(1H-pyrrol-2-yl)methanone (1)

Benzoylmorpholine (4.7 g, 2.5 mmol) and 4.5 ml $POCl_3$ were added in 50-mL round-bottom flask. The mixture was heated to 50 °C for 30 min, chilling the solutions to room temperature and then stirring 5 h. Pyrrole (0.5 ml, 7.72 mmol), with 10 ml anhydrous CH_2Cl_2 was dropped into the reaction mixture, and mixture was further stirring for overnight. After reaction was completed, saturated sodium hydroxide was added until pH = 7. The reaction solution was extracted with CH_2Cl_2 (50 mL × 3), dried over Na_2SO_4, and evaporated. The residue was purified by column chromatography (silica gel, (10:1, v/v) ethyl acetate/petroleum ether) to give **1** (3.14 g, 75 %) as a yellow crystalline solid. ^{1}H NMR (400 MHz, $CDCl_3$) δ 9.72 (s, 1H),

7.90 – 7.76 (m, 2H), 7.50 (t, J = 6.8 Hz, 1H), 7.09 (td, J = 2.7, 1.3 Hz, 1H), 6.84 – 6.82 (m, 1H), 6.65 – 5.71 (m, 1H).

Synthesis of (5-chloro-1H-pyrrol-2-yl)(phenyl)methanone (2)

Compound 1 (3 g, 17.5 mmol) and $CuCl_2.2H_2O$ (6 g, 35 mmol) were dissolved in 90 ml anhydrous CH_3CN, and the reaction mixture was stirred at 85 °C for 12 hours. After the reaction was completed, the reaction mixture was cooled to room temperature and poured into saturated NaCl solution, and resulting mixture was extracted with DCM (50 mL × 3). The combined organic layer was dried with Na_2SO_4 and concentrated under reduced pressure. The crude product was purified by silica gel chromatography (silica gel, (50:1, v/v) ethyl acetate/petroleum ether) to give **2** (1.1 g, 30.5 %) as a colorless solid. 1H NMR (400 MHz, $CDCl_3$) δ 10.10 (s, 1H), 7.88 (d, J = 7.5 Hz, 2H), 7.64 – 7.56 (m, 2H), 7.49 (t, J = 7.5 Hz, 3H), 6.85 – 6.81 (m, 1H), 6.24 – 6.18 (m, 1H).

Synthesis of 3-chloro-5,7-dimethyl-6-ethyl-8-phenyl-BODIPY (4).

To a solution of anhydrous CH_2Cl_2 (25 mL) in 50-mL round-bottom flask, (0.55 g, 2.68 mmol) compound 2 and 0.75 ml $POCl_3$ were added. The solution was cooled to 0 °C and stirring for 30 min. Then, a solution of 3-Ethyl-2,4-dimethylpyrrole (1.0 g, 10 mmol) in dry CH_2Cl_2 (5 mL) was slowly added through a constant pressure drop of liquid funnel, and the mixture was stirred at room temperature for 12 h. Aqueous $NaHCO_3$ (50mL) was poured into the mixture solutions, dried with anhydrous Na_2SO_4, and concentrated under vacuum to obtained compound 3. Without further purified, the residue was dissolved in anhydrous (50mL) CH_2Cl_2, 1ml Et_3N was added into the solution and stirred for 1h at room temperature. Then, $BF_3 \cdot OEt_2$ (0.9 mL, 6.62 mmol) was slowly dropped into the mixture and stirred at room temperature overnight. After reaction was completed, concentrated under vacuum and the rude product was purified by silica gel chromatography (silica gel, (20:1, v/v) ethyl acetate/petroleum ether) to give **4** (0.28 g, 29.8 %) as obtained orange powdery solid. ^{1}H NMR (400 MHz, $CDCl_3$) δ 7.56 – 7.43 (m, 3H), 7.35 – 7.29 (m, 2H), 6.24 (d, J = 3.8 Hz, 1H), 6.20 (d, J = 3.8 Hz, 1H), 2.63 (s, 3H), 2.35 (q, J = 7.6 Hz, 2H), 1.43 (s,

3H), 1.05 – 1.00 (t, J = 7.6 Hz, 3H).

Synthesis of 2-carbaldehyde-3-chloro-5,7-dimethyl-6-ethyl-8-phenyl-BODIPY (5)

To a solution of anhydrous DMF (2 mL) in 25-mL round-bottom flask, 2 mL $POCl_3$ was added and stirred at 0°C for 30 min. After being warmed to room temperature, mixture was stirred for additional 30 min. Compound 4 (200 mg, 0.52 mmol) was dissolved in 10 ml anhydrous CH_2Cl_2 and slowly dropped into the mixture. Under ambient temperature the mixture was stirred for 36 h. After the reaction was completed, aqueous $NaHCO_3$ and NaOH was added into carefully, extracted with DCM (20 mL × 3). The organic layer was dried over Na_2SO_4 and concentrated under reduced pressure. The crude product was purified by silica gel chromatography (silica gel, (20:1, v/v) ethyl acetate/petroleum ether) to give **5** (80 mg, 37.0 %) as brown solid. ^{1}H NMR (400 MHz, $CDCl_3$) δ 9.86 (s, 1H), 7.68 – 7.42 (m, 3H), 7.34 – 7.29 (m, 2H), 6.64 (s, 1H), 2.70 (s, 3H), 2.39 (q, J = 7.6 Hz, 2H), 1.49 (s, 3H), 1.05 (t, J = 7.6 Hz, 3H).

Synthesis of compound (6)

In a clean dry flask, compound 5 (78 mg, 0.2 mmol) was dissolved in 20 mL anhydrous ethanol, 100 μL piperidine was added and heated to refluxed for 12 h. After removed solvent under reduced pressure, and the residue was purified by silica gel chromatography (silica gel, (10:1- 8:1, v/v) ethyl acetate/petroleum ether) to give pure compound 6 as grey powdery solid (32 mg, 33 %). ^{1}H NMR (400 MHz, $CDCl_3$) δ 9.72 (s, 1H), 7.62 – 7.38 (m, 4H), 7.36 – 7.28 (m, 2H), 6.76 (s, 1H), 3.68 – 3.61 (m, 4H), 2.59 (s, 3H), 2.36 (q, J = 7.6 Hz, 2H), 1.85 – 1.74 (m, 5H), 1.73 – 1.65 (m, 2H), 1.43 (s, 3H), 1.02 (t, J = 7.6 Hz, 3H). HRMS (ESI) calcd for $C_{25}H_{28}BF_2N_3O$ $[M + H]^+$: 436.2366, found: 436.2374.

Synthesis of compound (7)

In a 50-mL round-bottom flask, compound 6 (80 mg, 0.2 mmol) was dissolved in (20 mL) anhydrous ethanol, p-nitrobenzaldehyde (90 mg, 0.6 mmol) and 100 μL piperidine was added into the solution. The mixture was heated to reflux for 12 h. After cooled to room temperature, excess ethanol was removed under vacuum. The

residue was purified by silica gel chromatography (silica gel, (10:1- 8:1, v/v) ethyl acetate/petroleum ether) to give pure compound 7 as blue solid (19 mg 16.3 %)。^{1}H NMR (400 MHz, CDCl3) δ 9.70 (s, 1H), 8.25 (d, J = 8.8 Hz, 2H), 7.89 (d, J = 16.8 Hz, 1H), 7.70 (d, J = 3.5 Hz, 1H), 7.56 – 7.45 (m, 3H), 7.36 – 7.29 (m, 2H), 7.22 (d, J = 16.8 Hz, 1H), 6.97 (s, 1H), 3.84 – 3.73 (m, 4H), 2.65 (q, J = 7.5 Hz, 2H), 1.94 – 1.80 (m, 4H), 1.79 – 1.69 (m, 2H), 1.46 (s, 3H), 1.19 (t, J = 7.5 Hz, 3H). HRMS (ESI) calcd. for $C_{32}H_{31}BF_2N_4O_3$ $[M + H]^+$: 569.2530, found: 569.2540.

Synthesis of compound (8)

Compound 6 (40 mg, 0.1 mmol), 3,4-dimethoxybenzaldehhyde (50 mg, 0.3 mmol) and 100 μL piperidine dissolved in (20 mL) anhydrous ethanol was added into 50-mL round-bottom flask. The mixture was heated to reflux for 12 h and then cooled to room temperature. Excess ethanol was removed under vacuum, and the residue was purified by silica gel chromatography (silica gel, (10:1-8:1-6:1, v/v) ethyl acetate/petroleum ether) to give pure compound 8 as dark blue solid (10.7 mg 21.3 %). ^{1}H NMR (400 MHz, $CDCl_3$) δ 9.72 (s, 1H), 7.66 (d, J = 16.7 Hz, 1H), 7.53 – 7.44 (m, 3H), 7.34 – 7.30 (m, 2H), 7.23 (d, J = 16.7 Hz, 1H), 7.18 (dd, J = 8.3, 1.9 Hz, 1H), 7.14 (d, J = 1.9 Hz, 1H), 6.91 (d, J = 8.3 Hz, 1H), 6.81 (s, 1H), 3.96 (d, J = 17.8 Hz, 6H), 3.76 – 3.68 (m, 4H), 1.86 – 1.77 (m, 4H), 1.75 – 1.68 (m, 2H), 1.45 (s, 3H), 1.19 (t, J = 7.5 Hz, 3H). HRMS (ESI) calcd for $C_{34}H_{36}BF_2N_3O_3$ $[M + H]^+$: 584.2891, found: 584.2896.

Synthesis of compound (9)

Compound 6 (40 g, 0.1 mmol) and p-dimethylaminobenzaldehyde (47 mg, 0.3 mmol) were dissolved in 20 ml anhydrous ethanol, and then100 μL piperidine was added into the mixture. Reaction mixture was stirred at 85 °C for 12 hours. After the reaction was completed, excess ethanol was removed under reduced pressure, and the residue was purified by silica gel chromatography (silica gel, (10:1-8:1-6:1, v/v) ethyl acetate/petroleum ether) to give pure compound 9 as blue solid (10.7 mg 16.2 %).^{1}H NMR (400 MHz, $CDCl_3$) δ 9.66 (s, 1H), 7.56 (d, J = 16.7 Hz, 1H), 7.46 (t, J = 6.9 Hz, 3H), 7.39 (d, J = 6.8 Hz, 3H), 7.23 (d, J = 6.2 Hz, 3H), 6.73 (s, 1H), 6.65 (s, 1H), 3.60

(m, 4H), 2.99 (s, 6H), 2.58 (d, J = 7.4 Hz, 2H), 1.71 (d, J = 22.7 Hz, 4H), 1.68 – 1.56 (m, 2H), 1.37 (s, 3H), 1.11 (t, J = 7.4 Hz, 3H). HRMS (ESI) calcd for $C_{34}H_{38}BF_2N_4O$ $[M + H]^+$: 567.3101, found: 567.3110.

Synthesis of 1-ethylbenzo[cd]indol-2(1H)-one (2.1)

1,8-naphtholactam (0. 5 g, 3 mmol) and potassium hydroxide (0.56 g, 10 mmol) were dissolved in DMF and the mixture was stirred at 30 °C for 10 min. Then, (0.75 ml 10 mmol) CH_3CH_2I was introduced into the solution. The reaction was heated at 90 ^oC for 10 h. After cooling to room temperature, the solution was poured into 100 ml ice water, and precipitate was collected by filtration. The product was pure enough to carry out the next reaction directly.

Synthesis of 1-ethyl-2-methyl-benz[c,d] indolium salts

A solution of **2.1** (0.5 g, 2.5 mmol) and Methyl magnesium chloride (3.0 M solution in tetrahydrofuran (THF), 1 mL, 3 mmol) dissolved in anhydrous THF (20 mL) was stirred at 55 °C for 1 h under a nitrogen atmosphere. After reaction was completed, mixture was cooled down, neutralized by addition of 1M hydrochloric acid and saturated potassium iodide solution to obtained orange solid (0.37 g 75 %). ^1H NMR (400 MHz, DMSO) δ 8.99 (d, J = 6.3 Hz, 1H), 8.81 (d, J = 7.6 Hz, 1H), 8.67 – 8.50 (m, 1H), 8.46 (d, J = 7.7 Hz, 1H), 8.21 – 8.09 (m, 1H), 8.06 – 7.94 (m, 1H), 4.73 (q, J = 7.1 Hz, 2H), 4.19 (s, 3H), 1.56 (t, J = 7.3 Hz, 3H). ^{13}C NMR (101 MHz, DMSO) δ 139.08 (s), 135.64 (s), 131.49 (s), 131.41 (s), 130.25 (s), 129.44 (s), 124.43 (s), 121.46 (s), 120.49 (s), 106.06 (s), 42.55 (s), 34.89 (s), 15.31 (s).

Synthesis of compound WD-CH_3

Compound 6 (12.3 mg, 0.02 mmol) and 1-ethyl-2-methylbenzo[cd]indol-1-ium (10 mg, 0.03 mmol) were dissolved in 20 mL absolute EtOH. The reaction mixture was heated to refluxed for 2 h. The solution was removed under reduced vacuum. The crude compound was purified by silica gel flash chromatography (silica gel, 100:1-50:1 v/v CH_2Cl_2/MeOH) to afford compound WD-CH_3 (11 mg 61%). ^1H NMR (400 MHz, $CDCl_3$) δ 8.42 (d, J = 7.4 Hz, 1H), 8.33 (d, J = 14.9 Hz, 1H), 8.26 (d, J = 8.1 Hz, 1H), 7.95 – 7.81 (m, 3H), 7.70 (t, J = 7.0 Hz, 1H), 7.63 – 7.52 (m, 3H),

7.40 – 7.30 (m, 2H), 7.03 (d, J = 14.8 Hz, 1H), 6.85 (s, 1H), 4.67 (q, J = 7.1 Hz, 2H), 3.83 – 3.58 (m, 4H), 2.59 (s, 2H), 2.34 (q, J = 7.6 Hz, 2H), 1.90 – 1.71 (m, 6H), 1.49 (t, J = 7.2 Hz, 3H), 0.99 (t, J = 7.6 Hz, 3H). HRMS (ESI) calcd for $C_{34}H_{38}BF_2N_4O^+$: 613.3309, found: 613.3322.

Synthesis of compound WD-OCH$_3$

In a 50 mL round-bottom flask, compound 8 (22.8 mg, 0.03 mmol) and 1-ethyl-2-methylbenzo[cd]indol-1-ium (15 mg, 0.045 mmol) were dissolved in 20 mL absolute EtOH. The reaction mixture was refluxed for 2 h. The solution was then removed to give the crude product. Crude compound was purified by silica gel flash chromatography (silica gel, 100:1-50:1 v/v CH_2Cl_2/MeOH) to afford compound WD-OCH$_3$ (18.1 mg 57 %). ^{1}H NMR (400 MHz, $CDCl_3$) δ 8.43 (d, J = 7.4 Hz, 1H), 8.33 (d, J = 14.8 Hz, 1H), 8.25 (d, J = 8.1 Hz, 1H), 7.93 (t, J = 7.3 Hz, 1H), 7.89 – 7.85 (m, 1H), 7.74 – 7.58 (m, 2H), 7.58 – 7.55 (m, 3H), 7.41 – 7.30 (m, 3H), 7.17 (d, J = 1.9 Hz, 1H), 7.10 (d, J = 1.8 Hz, 1H), 7.00 (d, J = 14.8 Hz, 1H), 6.90 – 6.84 (m, 1H), 4.65 (q, J = 7.5 Hz ,2H), 3.91 (d, J = 15.2 Hz, 6H), 3.78 (d, J = 5.3 Hz, 4H), 2.63 (q, J = 7.5 Hz, 2H), 1.81 (m, , 6H), 1.49 (t, J = 7.1 Hz, 3H), 1.42 (s, 3H), 1.15 (t, J = 7.6 Hz, 3H). HRMS (ESI) calcd for $C_{48}H_{48}BF_2N_4O_2^+$: 761.3833, found: 761.38275

Synthesis of compound WD-NME$_2$

Compound 9 (22.2 mg, 0.03 mmol) and 1-ethyl-2-methylbenzo[cd]indol-1-ium (15 mg, 0.045 mmol) were dissolved in 20 mL absolute EtOH. The reaction mixture was heated to refluxed for 2 h. After removal of the solvent, the crude product was purified by silica gel flash chromatography (silica gel, 100:1-50:1 v/v CH_2Cl_2/MeOH) to afford compound WD-NME$_2$ (16.2 mg, 55%). ^{1}H NMR (400 MHz, $CDCl_3$) δ 8.38 (d, J = 7.4 Hz, 1H), 8.32 (d, J = 14.6 Hz, 1H), 8.22 (d, J = 8.1 Hz, 1H), 7.96 – 7.88 (m, 1H), 7.84 – 7.77 (m, 2H), 7.68 (d, J = 7.6 Hz, 1H), 7.66 – 7.61 (m, 1H), 7.57 – 7.54 (m, 3H), 7.53 – 7.49 (m, 2H), 7.47 (d, J = 3.3 Hz, 1H), 7.45 (d, J = 2.1 Hz, 1H), 7.38 – 7.31 (m, 2H), 6.83 (d, J = 14.7 Hz, 1H), 6.74 (s, 1H), 6.62 (d, J = 11.6 Hz, 1H), 4.57 (q, J = 7.1 Hz, 2H), 3.76 (d, J = 5.3 Hz, 4H), 2.64 (q, J = 7.5 Hz, 2H), 1.89 – 1.78 (m, 6H), 1.47 (t, J = 6.9 Hz, 3H), 1.40 (s, 3H), 1.15 (t, J = 7.5 Hz, 3H).HRMS (ESI)

calcd for $C_{48}H_{48}BF_2N_4O_2^+$: 740.4044. Found: 740.40399

Synthesis of compound WD-NO_2

Compound 7 (22.4 mg, 0.03 mmol) and 1-ethyl-2-methylbenzo[cd]indol-1-ium (15 mg, 0.1 mmol) were dissolved in 20 mL anhydrous EtOH. The reaction mixture was the reaction was refluxed and stirred at 90 °C for 2 h. Excess solvent was removed through reduced pressure, and residue was purified by silica gel flash chromatography (silica gel, 100:1-50:1 v/v CH_2Cl_2/MeOH) to afford compound WD-NO_2 (18.8 mg 58%). ^{1}H NMR (400 MHz, $CDCl_3$) δ 8.57 (d, J = 7.3 Hz, 1H), 8.36 (d, J = 8.0 Hz, 2H), 8.29 (d, J = 8.8 Hz, 2H), 8.03 (d, J = 7.6 Hz, 1H), 7.98 (d, J = 8.0 Hz, 2H), 7.90 (d, J = 16.8 Hz, 1H), 7.80 (d, J = 7.6 Hz, 1H), 7.76 (d, J = 8.8 Hz, 2H), 7.64 (s, 3H), 7.46 (d, J = 3.5 Hz, 2H), 7.38 (d, J = 16.7 Hz, 2H), 7.24 (s, 1H), 4.84 (q, J = 16.7 Hz 2H), 3.87 (m, 4H), 2.69 (q, J = 7.4 Hz, 2H), 1.90 (m, 6H), 1.51 (s, 3H), 1.44 – 1.39 (t, J = 13.4 Hz 3H), 1.22 (t, J = 15.3 Hz, 4H).

^{13}C NMR (101 MHz, CD_2Cl_2/CD_4OD) δ 165.07 (s), 161.00 (s), 155.13 (s), 149.22 (s), 145.69 (s), 144.34 (s), 142.85 (s), 140.65 (s), 140.27 (s), 139.14 (s), 137.70 (s), 137.32 (s), 136.89 (s), 134.89 (s), 132.61 (s), 131.93 (s), 131.42 (s), 131.26 (s), 130.88 (s), 130.32 (s), 129.42 (s), 125.61 (s), 117.12 (s), 110.50 (s), 67.20 (s), 42.74 (s), 31.06 (s), 28.21 (s), 25.23 (s), 19.82 (s), 16.29 (s), 14.97 (s), 13.25 (s). HRMS (ESI) calcd for $C_{46}H_{43}BF_2N_5O_2^+$: 746.3472, found: 746.3480.

Theoretical calculations

Theoretical calculations were performed to further understand the viscosity sensing mechanism. Based on the density functional theory (DFT), the values of the rotatable dihedral angle between BODIPY fluorophore and 1-ethyl-2-methyl-benz[c,d] iodolium salt, related charge density on connecting bonds as well as the geometry for molecular ground-state were carried out at the B3LYP/ 6-31G* level. In addition, to verify that the Nitro (electron-withdrawing) and Methoxy & Diethylamino (electron-donating groups) were participated in the π-conjugation and extended the bathochromic shift of absorption and fluorescence emission, frontier molecular orbital plots, including the energy levels for highest occupied molecular orbital (HOMO) and

lowest unoccupied molecular orbital (LUMO) of **WD-X** were carried out with the time dependent DFT (TDDFT) with the optimized structure of the ground (DFT/6-31G(d)). All data were collected using the Gaussian 09 software.

Optical experiments

WD-X, including **WD-CH_3**, **WD-NO_2**, **WE-OCH_3** and **WD-NME_2** were dissolved in DMSO to prepare the stock solution with a concentration of 1 mM. Photophysical properties, such as absorption/emission spectra, were measured by adding the stock solution (10 μL, 1.0 mM) to 0.5 mL of various solvents (MeOH, EtOH, CH_3CN, Acetone, DMF, DMSO, CH_2Cl_2, H_2O/CH_3CN, Glycerol) to obtain the final concentration of 20 μM. For the viscosity determination, solvents with different viscosity were obtained by mixing ethanol and glycerol in different proportions. The value of viscosity was recorded by NDJ-8 rotational viscometer. Solutions of **WD-X** with different viscosity were prepared by adding the 10 μL of stock solution to 0.5 mL of mixture solvent (ethanol-glycerol) with the final concentration of 20.0 μM. These solutions were sonicated for 10 min to eliminate air bubbles. The absorption/emission spectra of the **WD-X** solutions with different viscosity were measured on a UV-vis-NIR spectrophotometer (Shimadzu UV-2550, Japan) and Near-II fluorescence spectrophotometer with 808 nm excitation wavelength at a constant temperature of 25 °C.

Determination of fluorescence quantum yields

The fluorescence quantum yields were determined by plotting the integrated fluorescence intensity vs absorbance value. In this work, the quantum yields of **WD-X** in various solvents were determined with the reference of IR 1061 (Φ = 1.7 % in CH_2Cl_2).[1] The quantum yields were calculated using the equation: $\Phi_{sam} = \Phi_{ref} \times (K_{sam}/k_{ref}) \times (n_{sam}/n_{ref})^2$, where, subscripts sam and ref denote test sample and reference, respectively. Φ is the fluorescence quantum yield, K is the slop of the plot, and n is the refractive index of the solvent. In order to maximize illumination homogeneity and optical transparency, all absorbance in tests were kept below 0.08 at 808 nm and the emission spectrum was collected in the range of 900-1400 nm.

The Förster-Hoffmann equation

According to the Forster-Hoffmann equation, the quantitative relationship between **WD-NO_2** and the solvent viscosity can be described as $\log(I) = c + x \log \eta$, where I is the fluorescence intensity at 982 nm, η is the viscosity, c is a constant, and x represents a probe-dependent constant.

Photostability, pH dependency and selectivity of probe

Firstly, the photostability of the **WD-X** compounds was investigated, using the commercially available dye ICG as a reference. Probes and ICG were dissolved in the mixture solution of PBS/CH_3CN (V/V = 1:1), and the final concentration was 20.0 μM. Under 808 nm laser at a fluency rate of 0.1 W/cm^2, the change of fluorescence intensity was recorded within 0-40 min. The emission intensity of **WD-X** and ICG was measured every 2.5 min. Then, to examine the selectivity of **WD-NO_2**, Cys, Hcy, GSH, H_2O_2, NO, HClO, $ONOO^-$, NTR, HSO_3^-, HS^-, Na_2S_2, Cu^{2+}, Zn^{2+}, Ca^{2+}, were individually added into the mixture solution of PBS/CH_3CN (V/V = 1:1) containing **WD-NO_2** (20.0 μM). In addition, to further assess the stability of probe to biological environments, **WD-NO_2** solutions of different pH values (4.32-8.05) were prepared by adding the stock solution of **WD-NO_2** (10 μL,1.0 mM) to 0.5 mL of various buffer solutions with different pH values to gain the final concentration of 20.0 μM. All the solutions were measured on Fluorolog-3 Near-II spectrofluorometer with excitation at 808 nm and emission spectra were collected at 870-1400 nm.

Cytotoxicity Assay.

MTT assay was performed to evaluate the cytotoxicity of probe **WD-NO_2**. HeLa cells were plated in 96-well plates and incubator for 24 h to adhere. Then, various concentrations of probe (0, 3, 5, 10, 15, 20, 25, 30 μM) were added into the media, and then incubated for another 24 h. Next, 10 μL of methylthiazolyl tetrazolium (MTT) (5 mg mL^{-1}) was added to each of the wells and incubated for 4 h, 100 μL DMSO was added to dissolve the formazan crystals. The absorbance was measured at 570 nm with Microplate Reader (Thermo Fisher Scientific, USA). The cell viability

was calculated as (%) = (OD570 (Experiments) – OD570 (Blank)) / (OD570 (Control) – OD570 (Blank)). All experiments were performed in 9 replicates. The cell viability was expressed by the average values ± standard deviation (SD).

Fluorescence imaging of viscosity in vivo

All animal procedures were performed in accordance with the Guidelines for Care and Use of Laboratory Animals of Wuhan University and approved by the Animal Ethics Committee of Wuhan University. Four-week old female Kunming mice were purchased from Hubei Provincial Center for Disease Control. All groups contained n = 3 mice. In order to verify **WD-NO_2** could be used for monitoring viscosity fluctuation in vivo, mice were divided into four groups and injected with monensin, nystatin or LPS respectively in abdomen to produce viscosity changing models. Before imaging, all mice were fasted for 12 hours for avoiding the possible impact of food fluorescence. In addition, the abdominal fur was removed by an electric shaver before imaging. The first group was intraperitoneally injected with **WD-NO_2** (100 100 μL of 1:20 DMSO/saline v/v, 0.3 mM) as the negative control. The second group was given an injection of monensin (0.5 mg/mL, 100 μL) into the peritoneal cavity followed by intraperitoneal injection of **WD-NO_2** (100 μL, 0.3 mM) after 24 hours. The mice in group c were intraperitoneally injected with nystatin (0.5 mg/mL, 100 μL), and 24 h later was loaded with **WD-NO_2** (100 μL, 0.3 mM). The mice in group d were intraperitoneally injected with LPS (1 mg/mL, 100 μL) followed by intraperitoneal injection of **WD-NO_2** (100 μL, 0.3 mM) 24 h later. Ex: 808 nm laser (50 mW/cm^2), exposure time: 200 ms, 1000 nm LP.

Monitoring viscosity in diabetes-induced liver injury

Four-week old female Kunming mice were purchased from Hubei Provincial Center for Disease Control. All groups for study contained n = 3 mice. After overnight fasting, the mice were intraperitoneally injected with STZ freshly dissolved in 0.01 mol/L citrate buffer (pH 4.5) at a dose of 150 mg/kg body weight to induce diabetic model. The diabetes of mice were confirmed by the presence of hyperglycemia (blood

glucose level ⩾ 16.7 mmol/L) 72 h after STZ injection and the level of blood glucose was detected by blood glucose meter. Once the model was determined to be successful, the mice were kindly kept during the next 7 days. Afterwards, all the diabetic mice were selected and divided into three groups. In the control group, normal mice were only i.v. injected with **WD-NO_2** (100 μL, 0.3 mM). In the experiment groups, diabetic mice were intraperitoneally injected with saline and resveratrol (RVT) at a dose of 10 mg/kg, as well as treated with oral metformin (Metf) at a dose of 100 mg/kg body weight for 7 consecutive days, respectively. Before imaging, the abdominal fur was removed by an electric shaver. Then, **WD-NO_2** (100μL, 0.3 mM) dissolved in DMSO/saline (v/v = 1：20) was intravenously injected into the mice. NIR-II imaging of the liver region was performed on an in vivo master with Ex=808 nm (50 mW/cm^2), exposure time: 200 ms, 1000 nm LP.

Scheme S1. Synthesis of WD-X and 1-ethyl-2-methyl-benz[c,d] indolium salts.

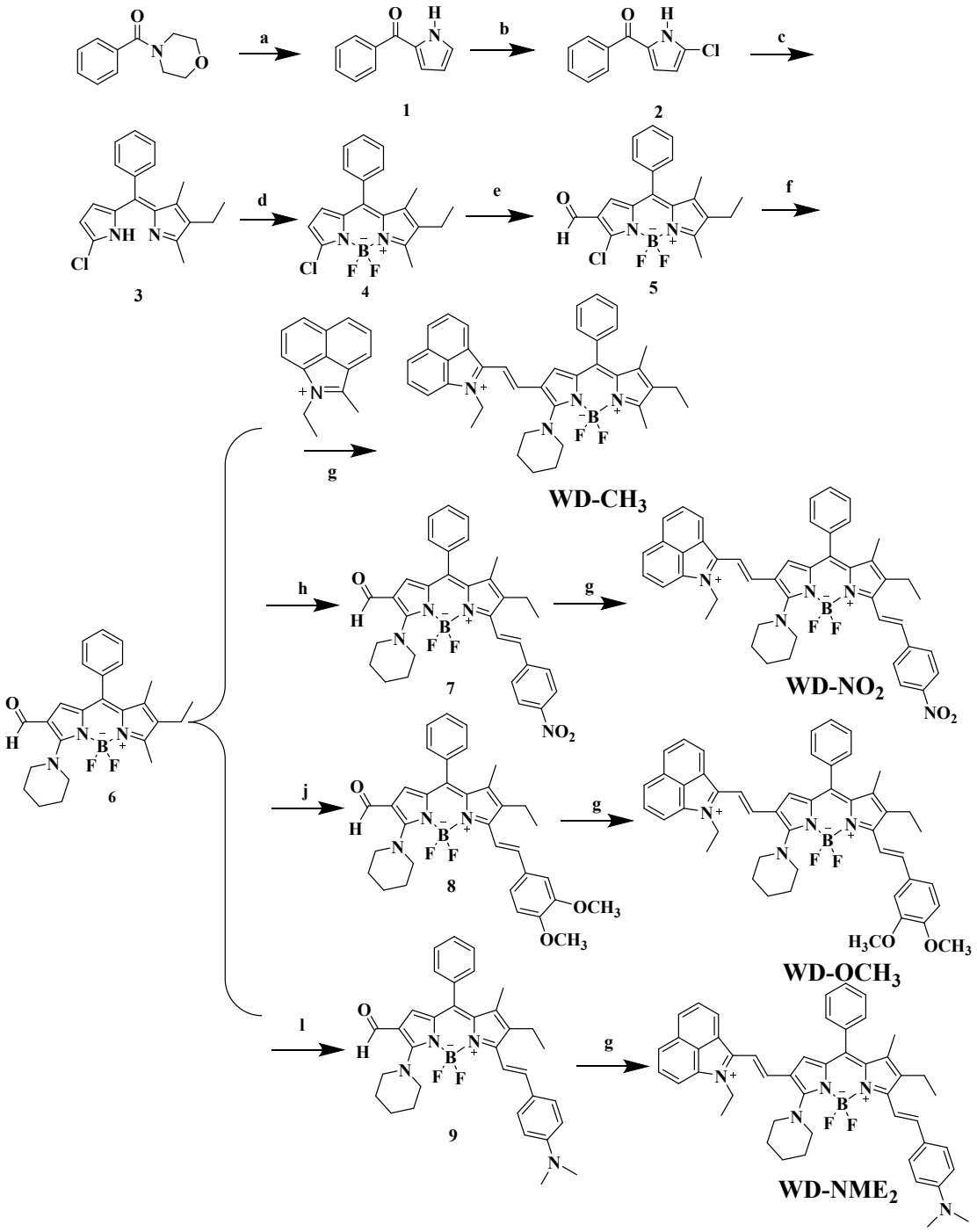

Synthesis of WD-X

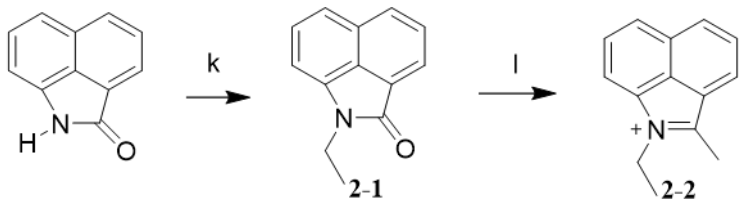

Synthesis of 1-ethyl-2-methyl-benz[c,d] indolium salts

a：$POCl_3$/pyrrole/CH_2Cl_2 b: $CuCl_2.2H_2O$/CH_3CN c: $POCl_3$/3-Ethyl-2,4-dimethylpyrrole/ CH_2Cl_2 d: Et_3N/BF_3 • OEt_2/CH_2Cl_2 e: DMF/$POCl_3$ f: pyridine/EtOH g: EtOH h: p-nitrobenzaldehyde/EtOH j: 3,4-dimethoxybenzaldehhyde/EtOH i: p-dimethylaminobenzaldehyde/EtOH k CH_3CH_2I/KOH/DMF l: CH_3MgBr/THF

Table S1. Reported representative fluorescent probes for monitoring viscosity

Probe	λabs (nm)	λex/nm	λem/nm	Stokes-shifts /nm	Bioimaging application
MCN[2]	400	400	470	70	cells, tissue & zebrafish
BMVC[3]	480	470	560	80	cells
Mito-V[4]	525	511	583	58	cells
NI-VIS[5]	550	560	670	120	cells, tissue & zebrafish
NLV-1[6]	680	650	719	69	cell，zebrafish, mice
WD-CH_3	755	808	1006	251	Mice (inflammation, diabetes)
WD-NO_2	809	808	1026	217	
WD-OCH_3	815	808	1052	237	
WD-NME_2	838	808	1100	262	

Figure S1. Structure and spatial configuration of representative (CH-1055, H1) and (CX-3, Flva7) fluorophores.

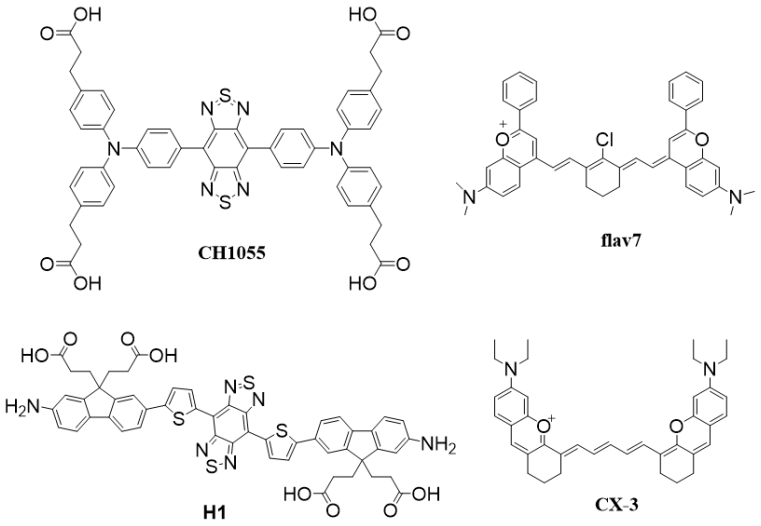

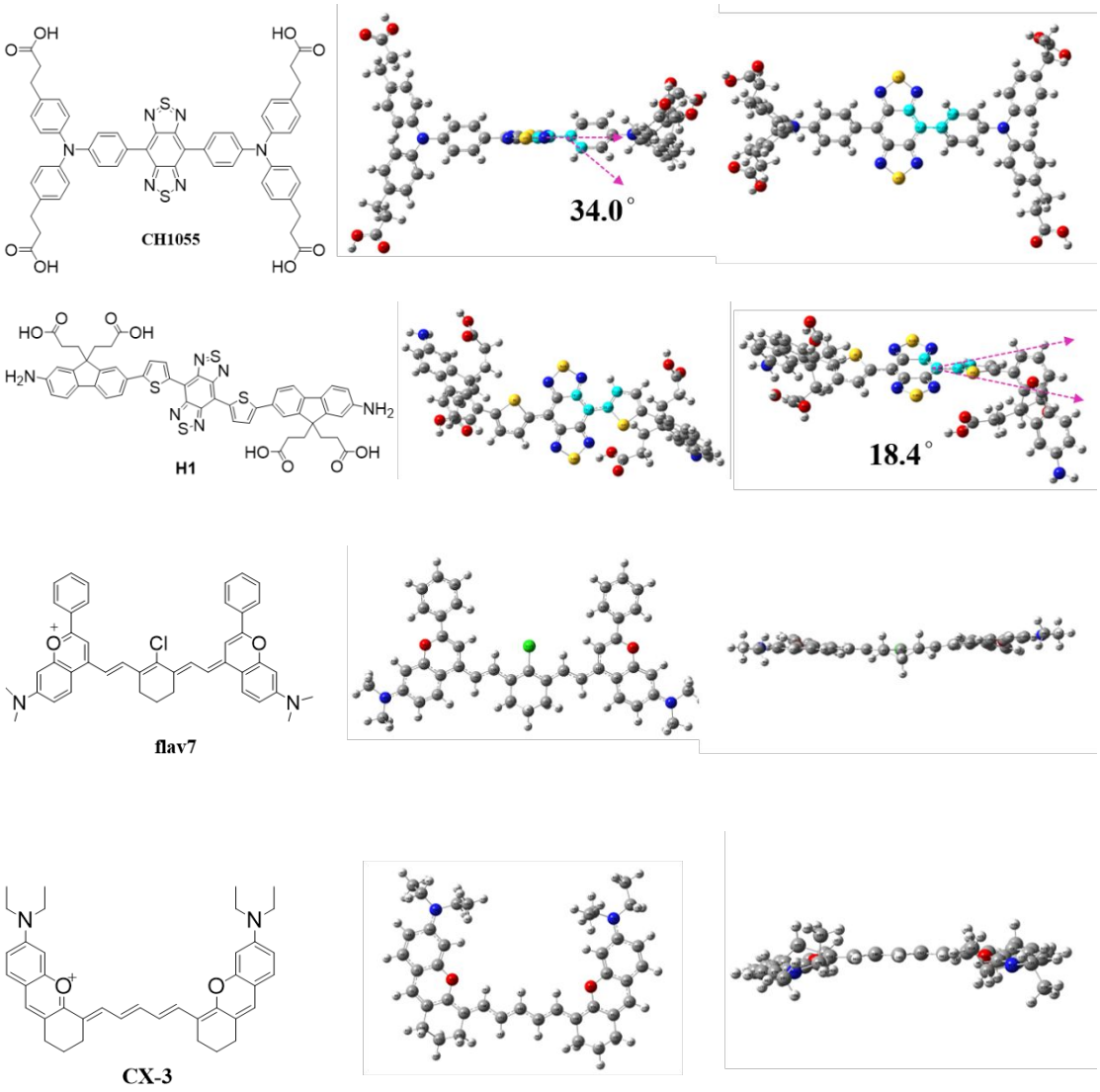

Figure S2 Viscosity response of CH-1055

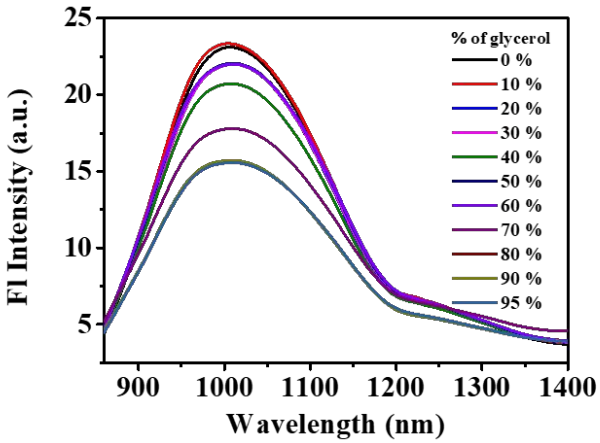

Figure S2. Fluorescence spectra of 10 μM CH-1055 in ethanol-glycerol systems at various ratios

Figure S3 Optical properties of WD-CH_3

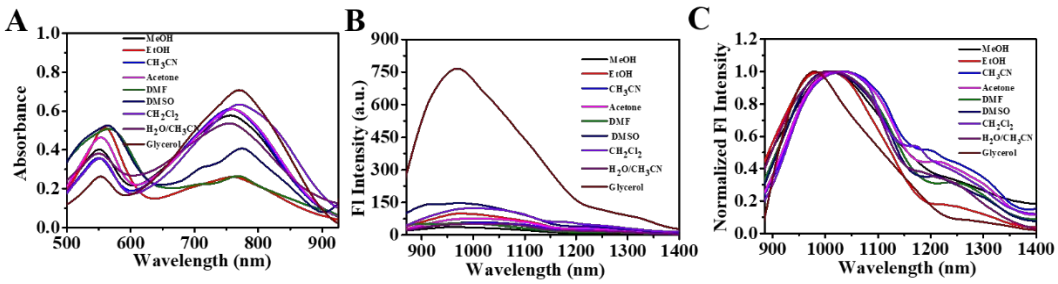

Figure S3. (A) UV-Vis-NIR spectra, fluorescence emission spectra (B) and normalized fluorescence intensity (C) of WD-CH_3 (20 μM) in different solvents.

Table S2. Photophysical properties of WD-CH_3

Dyes	solvents	λabs (nm)	ε ($M^{-1}cm^{-1}$)	λem (nm)	Stokes-shifts (nm)	Φ (%)
WD-CH_3	CH_3OH	757	28700	964	207	0.048
	EtOH	760	13200	978	218	0.208
	CH_3CN	756	31100	1024	268	0.074
	Acetone	760	30700	1010	250	0.090
	DMF	768	12700	982	214	0.186
	DMSO	775	18800	986	211	0.268
	CH_2Cl_2	770	31300	1000	230	0.141
	H_2O/CH_3CN	755	25700	1006	251	0.075
	Glycerol	768	36600	960	192	0.625

Figure S4 Optical properties of WD-NO_2

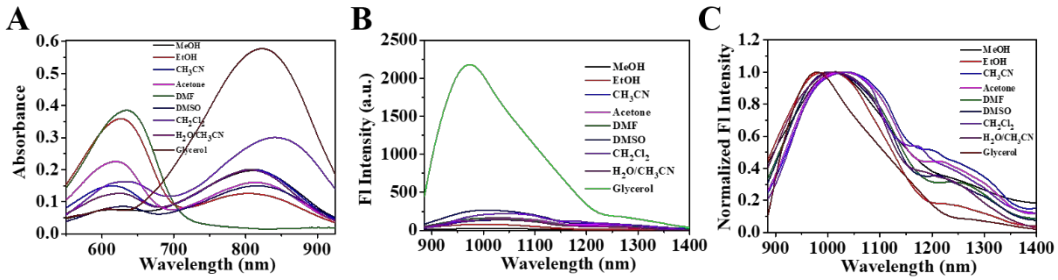

Figure S4. (A) UV-Vis-NIR spectra, fluorescence emission spectra (B) and normalized fluorescence intensity (C) of WD-NO_2 (20 μM) in different solvents. EX = 808 nm, emission spectra were collected at 880-1400 nm.

Table S3. Photophysical properties of WD-NO_2

Dyes	solvents	λabs (nm)	ε ($M^{-1}cm^{-1}$)	λem (nm)	Stokes-shifts (nm)	Φ (%)
WD-NO_2	CH_3OH	814	10700	1014	200	0.065
	EtOH	809	6500	1002	193	0.078
	CH_3CN	811	10700	1034	223	0.237
	Acetone	808	8700	1028	220	0.344
	DMF	817	ND	1010	195	ND[a]
	DMSO	815	7800	1008	193	0.568
	CH_2Cl_2	837	17300	1038	201	0.271
	H_2O/CH_3CN	809	10400	1026	217	0.230
	Glycerol	818	27600	982	164	1.662

a = not detected

Figure S5 Optical properties of WD-OCH_3

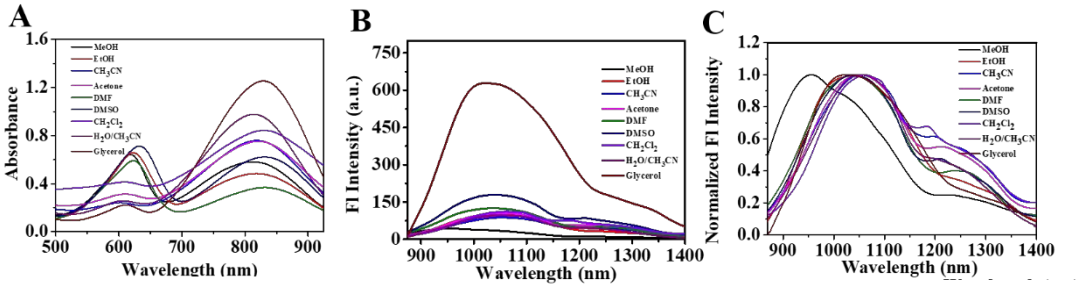

Figure S5. (A) UV-Vis-NIR spectra, Fluorescence emission spectra (B) and normalized fluorescence intensity (C) of WD-OCH_3 (20 μM) in different solvents.

Table S4. Photophysical properties of WD-OCH_3

Dyes	solvents	λabs (nm)	ε ($M^{-1}cm^{-1}$)	λem (nm)	Stokes-shifts (nm)	Φ (%)
WD-OCH_3	CH_3OH	812	28300	958	146	0.058
	EtOH	818	25300	1040	222	0.118
	CH_3CN	820	35800	1054	234	0.137
	Acetone	821	35200	1052	231	0.140
	DMF	831	18700	1042	211	0.232
	DMSO	831	31800	1040	209	0.194
	CH_2Cl_2	830	43900	1062	232	0.111
	H_2O/CH_3CN	815	47000	1052	237	0.069
	Glycerol	830	64800	1024	182	0.405

Figure S6 Optical properties of WD-NME_2

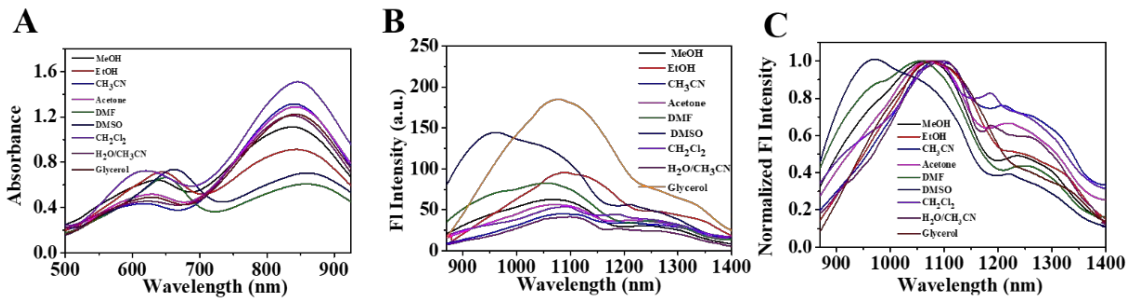

Figure S6. (A) UV-Vis-NIR spectra, fluorescence emission spectra (B) and normalized fluorescence intensity(C) of WD-NME_2 (20 μM) in different solvents.

Table S5. Photophysical properties of WD-NME_2

Dyes	solvents	λabs (nm)	ε ($M^{-1}cm^{-1}$)	λem (nm)	Stokes-shifts (nm)	Φ (%)
WD-NME_2	CH_3OH	839	55300	1068	229	0.048
	EtOH	843	45300	1074	231	0.075
	CH_3CN	841	65800	1088	247	0.031
	Acetone	842	64200	1070	228	0.039
	DMF	859	30700	1056	197	0.102
	DMSO	859	38800	974	115	0.104
	CH_2Cl_2	846	74900	1092	246	0.033
	H_2O/CH_3CN	838	60000	1100	262	0.029
	Glycerol	850	61600	1070	225	0.135

Figure S7 Frontier molecular orbital plots and HOMO, LOMO energy of WD-X

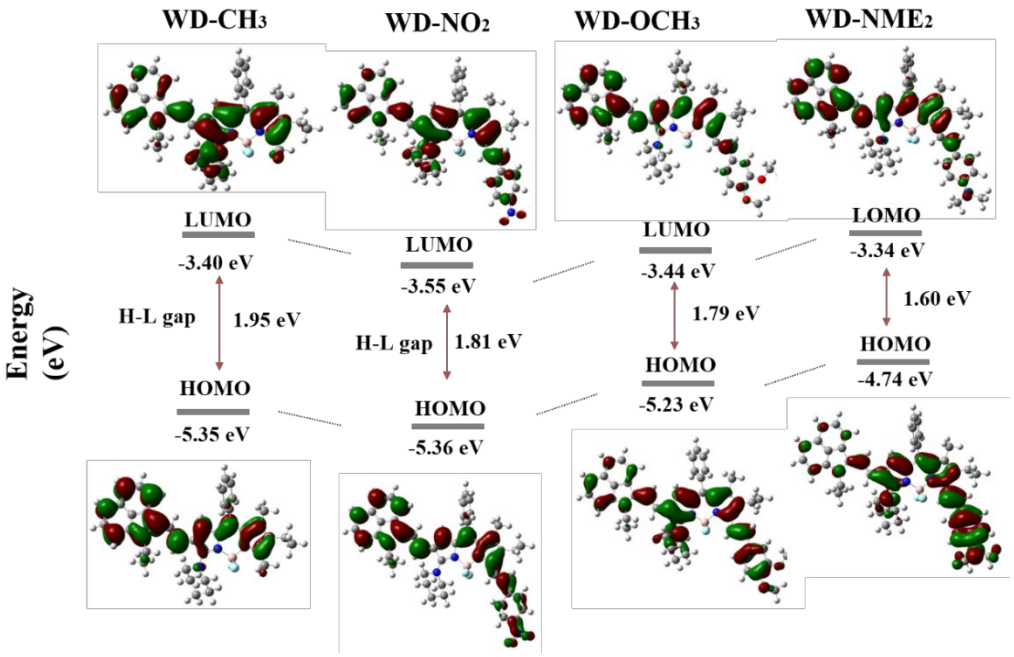

Figure S7. Frontier molecular orbital plots and HOMO, LOMO energy of **WD-X** (**WD-CH_3**, **WD-NO_2**, **WD-OCH_3**, **WD-NME_2**). Green and red shapes are corresponding to the different phases of the molecular wave functions for HOMO and LUMO orbitals.

Figure S8 Absorption and fluorescence spectra of WD-CH_3, WD-OCH_3 and WD-NME_2

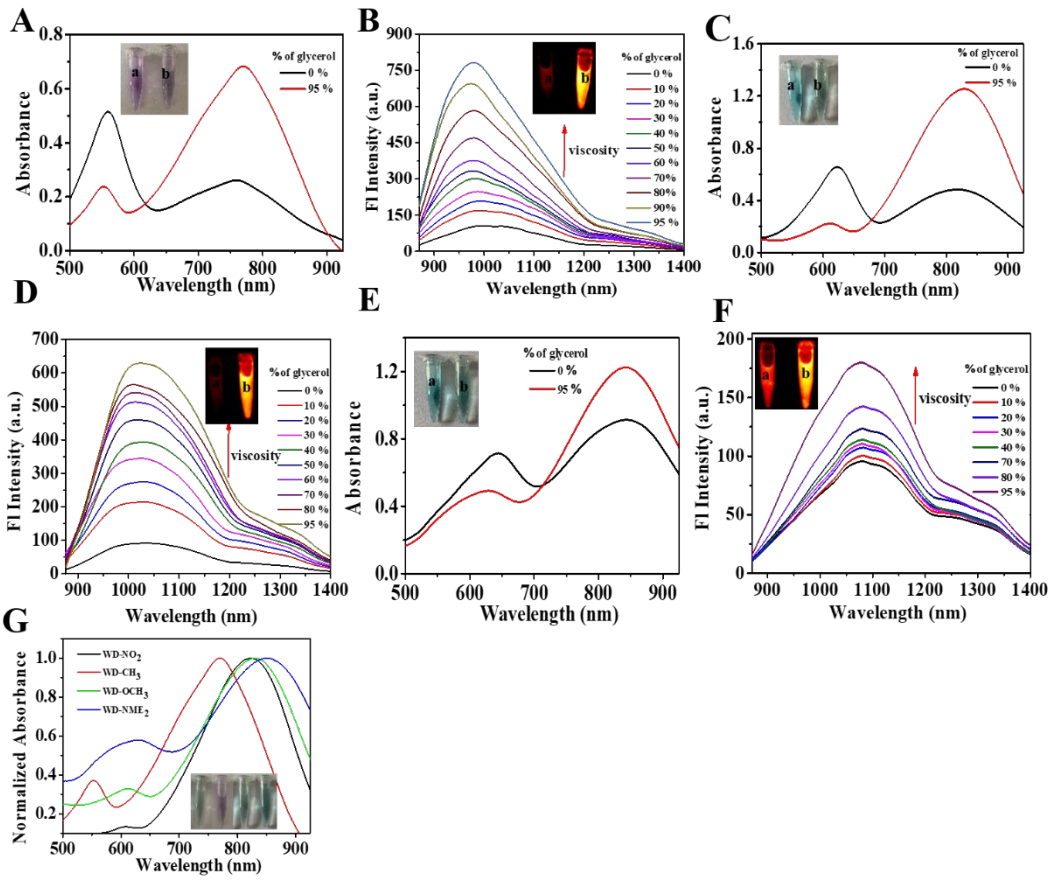

Figure S8. Absorption and fluorescence spectra of (20 μM) **WD-CH_3** (A-B), **WD-OCH_3** (C-D) and **WD-NME_2** (E-F) in ethanol and glycerol (95%); normalized absorbance of 20 μM **WD-X** (G) in glycerol (95%).

Figure S9 Investigation on the Specificity of WD-NO_2

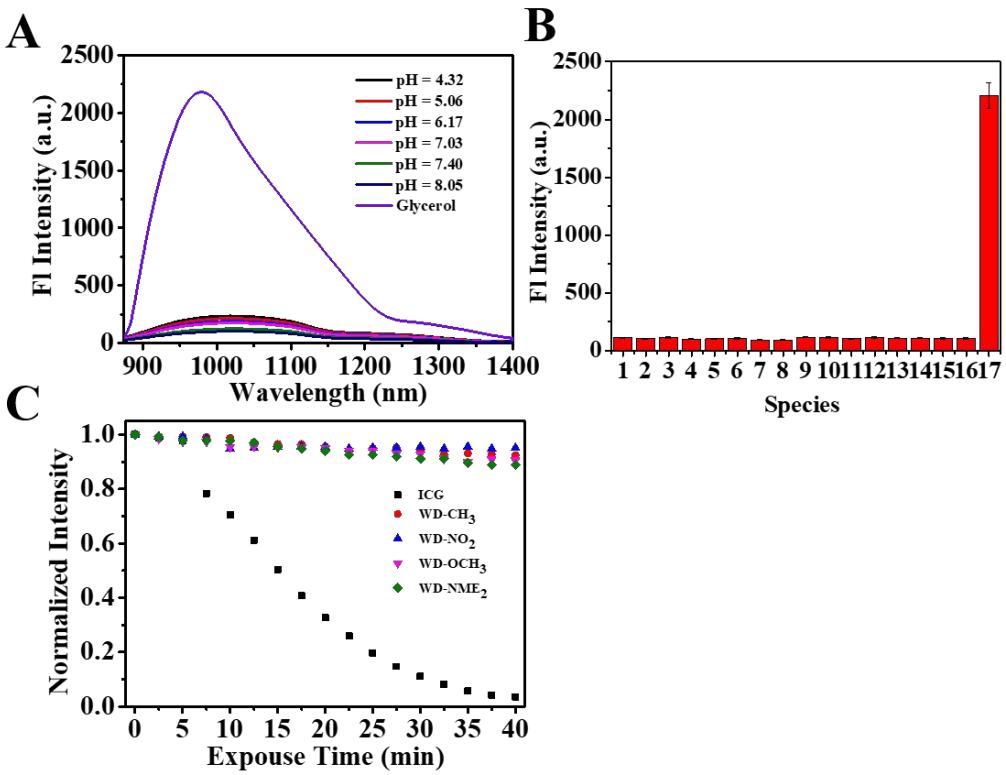

Figure S9. (A) Fluorescence intensity response of **WD-NO_2** (20 μM) carried out in phosphate buffered solution (10 mM) with different pH (4.32, 5.06, 6.17, 7.03, 7.40, 8.05). (B) Fluorescence response of **WD-NO_2** (20 μM) toward various species. For reactive sulfide species: Cys, Hcy and GSH (1 mM), HSO_3^- , HS^- and Na_2S_2 (100 μM). For reactive oxygen/nitrogen species: H_2O_2, NO, HClO, $ONOO^-$ (100 μM). K^+, Cu^{2+}, Zn^{2+}, Ca^{2+}, (1 mM), NTR (1 μg/mL) and 0.5 mM NADH. 1. ethanol; 2, Cys; 3, Hcy; 4, GSH; 5, H_2O_2; 6, NO; 7, HClO; 8, $ONOO^-$; 9, HSO_3^-; 10, HS^-; 11, Na_2S_2; 12, K^+; 13, Cu^{2+}; 14, Zn^{2+}; 15, Ca^{2+}; 16, NTR+ NADH; 17, glycerol. (C) Normalized emission decay of **WD-X** and ICG at their emission maximaum under laser irradiation (808 nm, 100 mW/cm^2) for different irradiation time.

Figure S10 Cytotoxicity of WD-NO_2

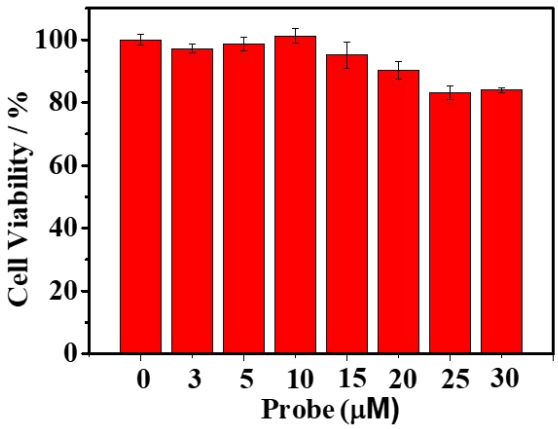

Figure S10. The MTT experiment of **WD-NO_2** with different concentrations (0 μM, 3 μM, 5 μM, 10 μM, 15 μM, 20 μM, 25 μM and 30 μM) for HeLa cells.

Figure S11. Fluorescence imaging of viscosity changes by exogenous drug stimulation.

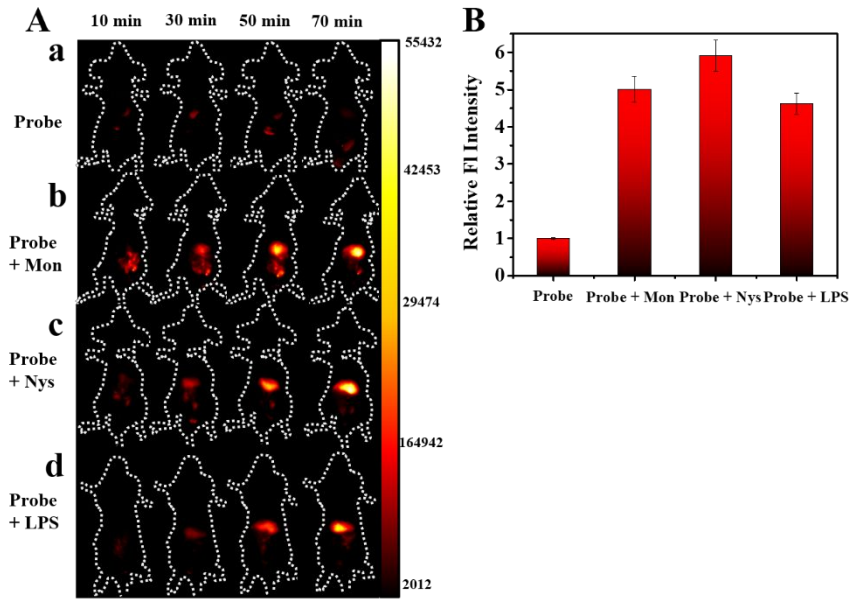

Figure S11. (A) Fluorescence imaging of viscosity changes by exogenous drug stimulation. (A-a) mice were only intraperitoneally injected with **WD-NO_2** (100 μL, 0.3 mM). In vivo imaging of livers of mice treated with various drugs: monensin

(A-b), nystatin (A-c) and LPS (A-d). All groups for study contained n = 3 mice. Ex: 808 nm laser (50 mW/cm^2), exposure time: 200 ms, 1000 nm LP. (B): Normalized relative fluorescence intensity of the above groups of mice.

Figure. S12 1H NMR of phenyl(1H-pyrrol-2-yl)methanone (1)

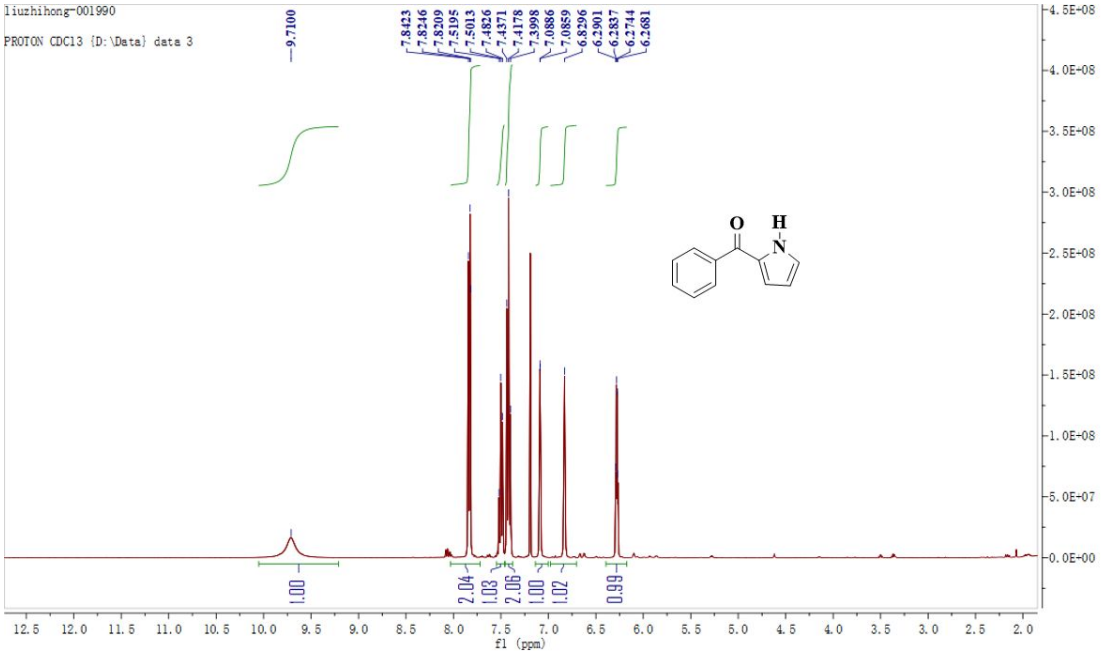

Figure.S13 ^{1}H NMR (5-chloro-1H-pyrrol-2-yl)(phenyl)methanone (2)

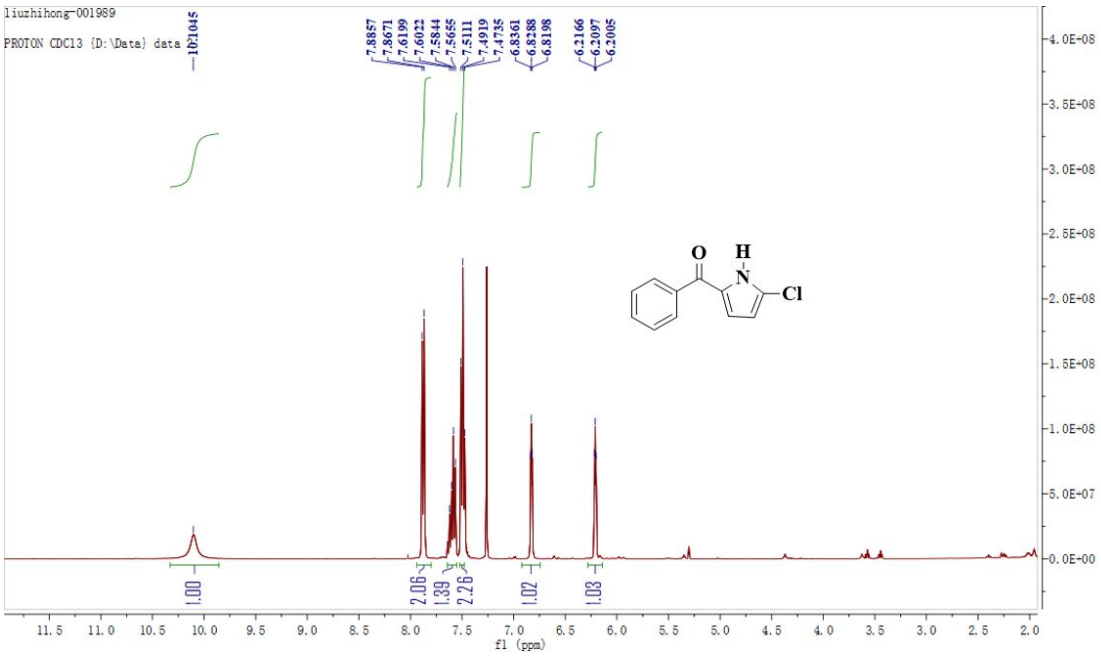

Figure.S14 ^{1}H NMR of 3-chloro-5,7-dimethyl-6-ethyl-8-phenyl-BODIPY (4).

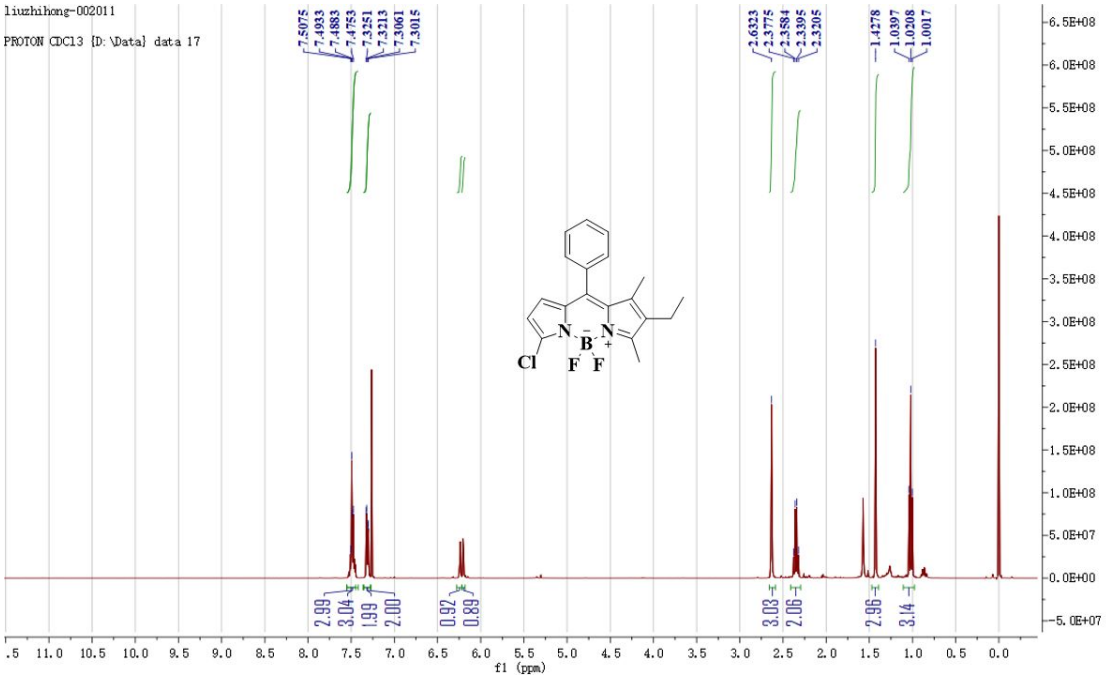

Figure.S15 ^{1}H NMR of 2-carbaldehyde -3-chloro- 5,7-dimethyl- 6-ethyl -8-phenyl -BODIPY (5)

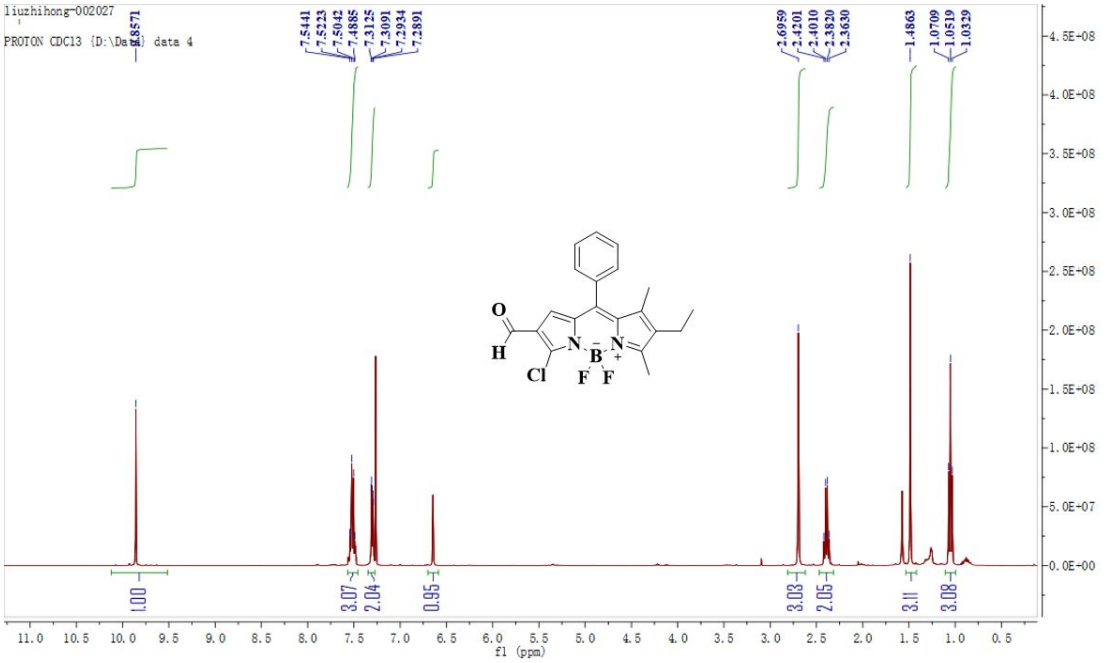

Figure.S16 ^{1}H NMR and HRMS of compound (6)

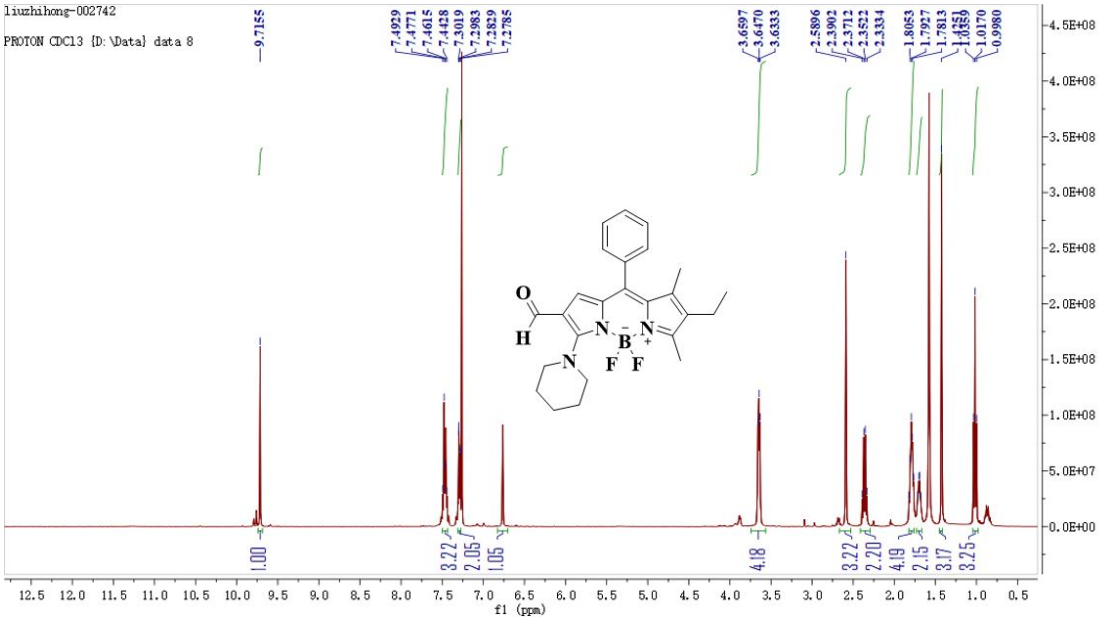

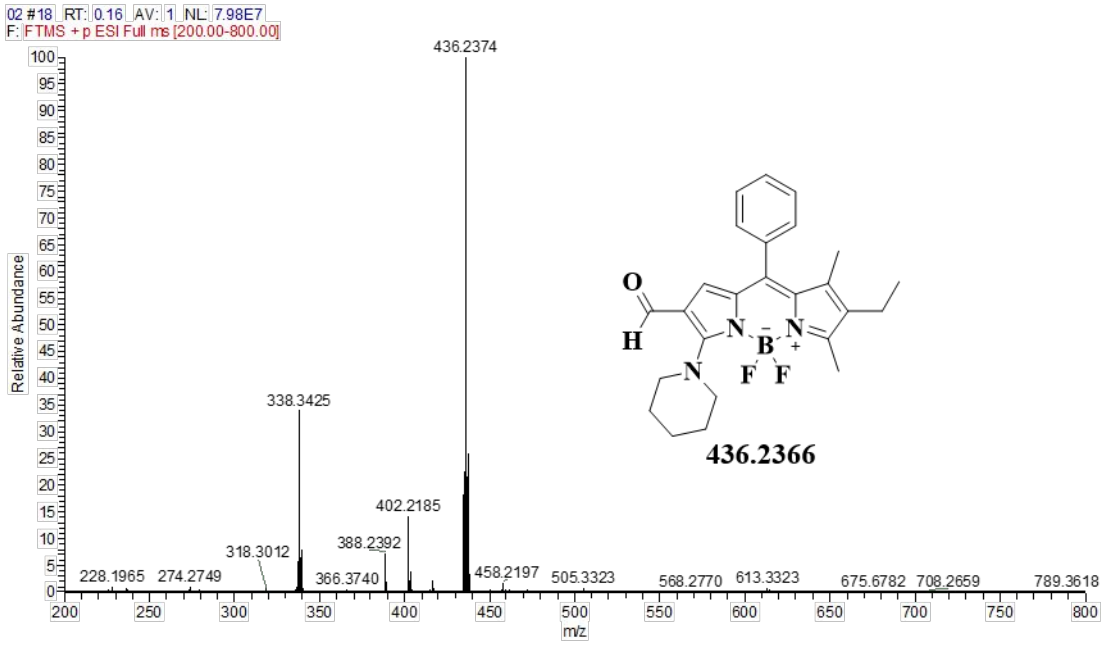

Figure.S17 ^{1}H NMR and HRMS of compound (7)

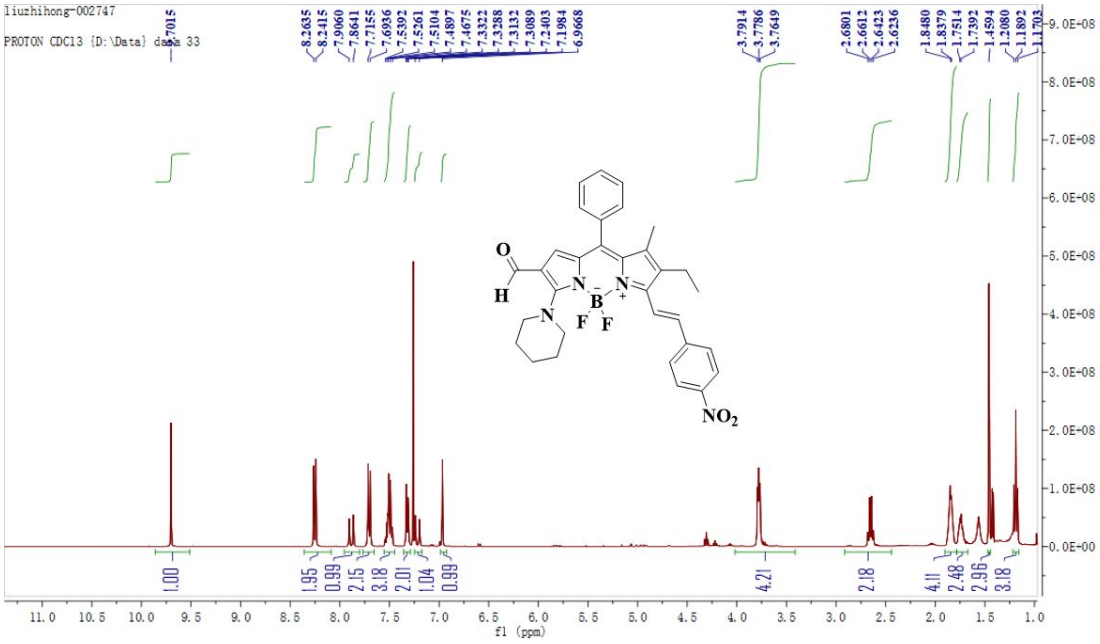

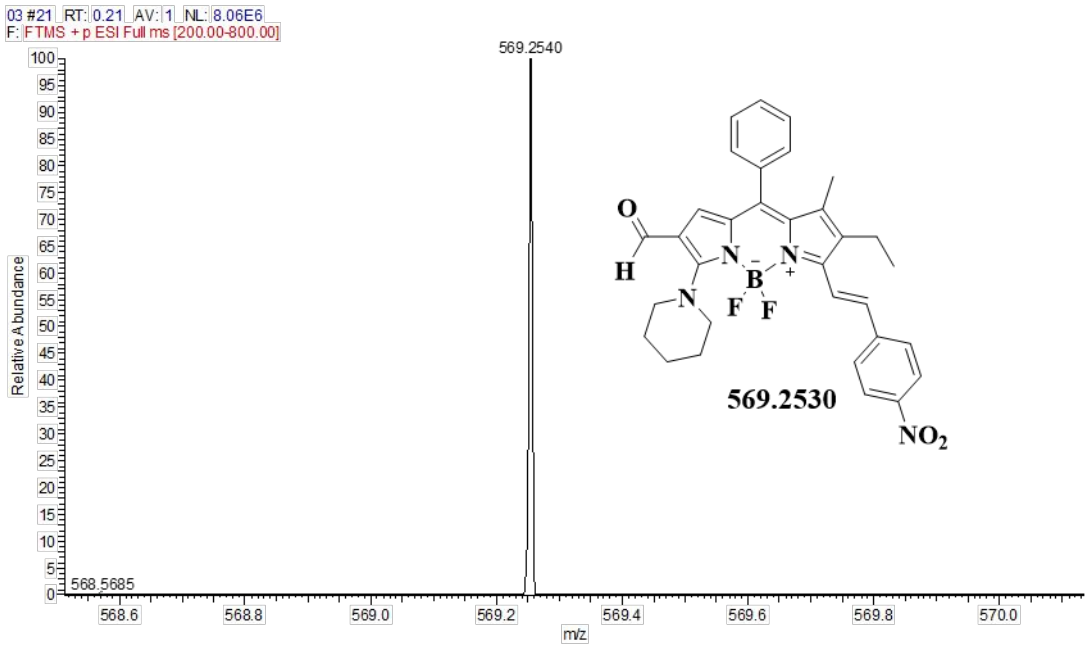

Figure.S18 ^{1}H NMR and HRMS of compound (8)

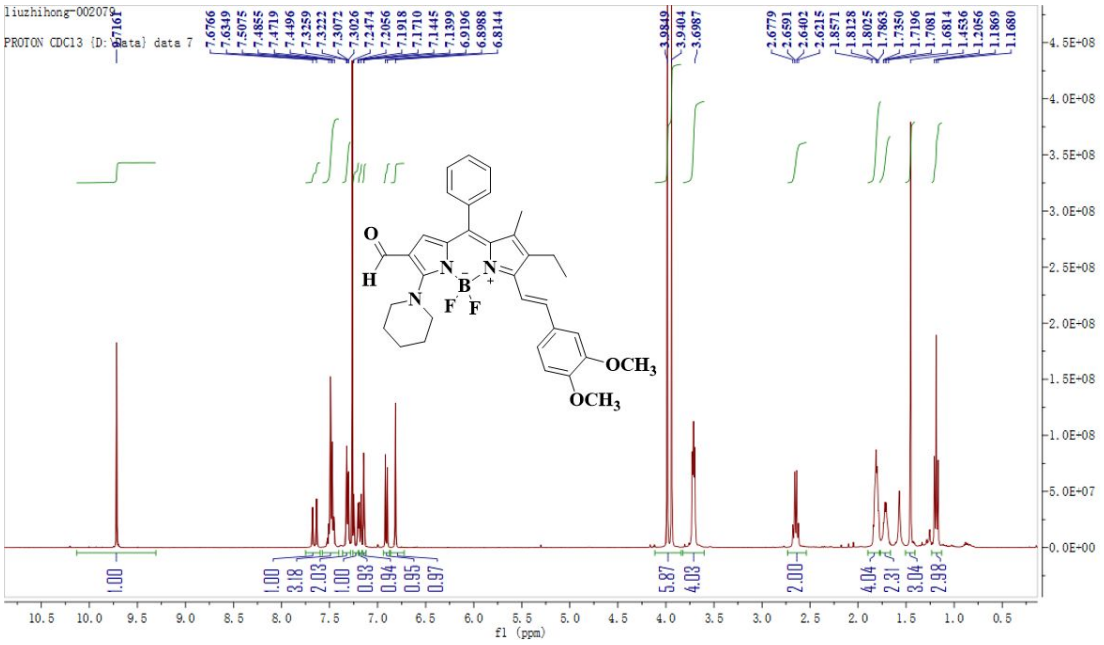

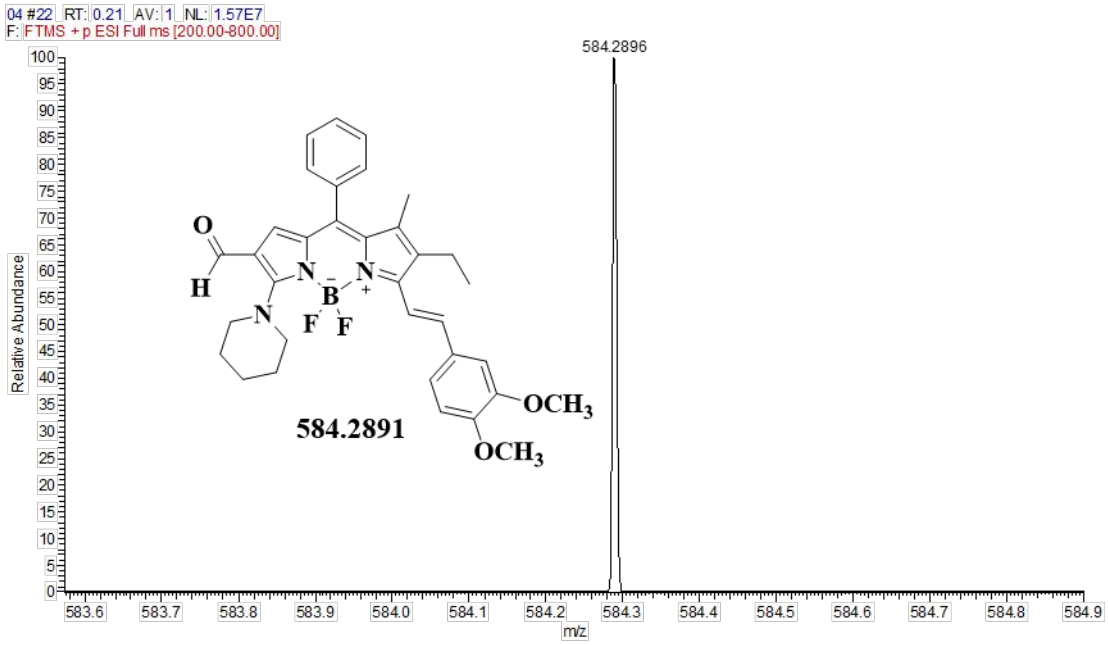

Figure.S19 ^{1}H NMR and HRMS of compound (9)

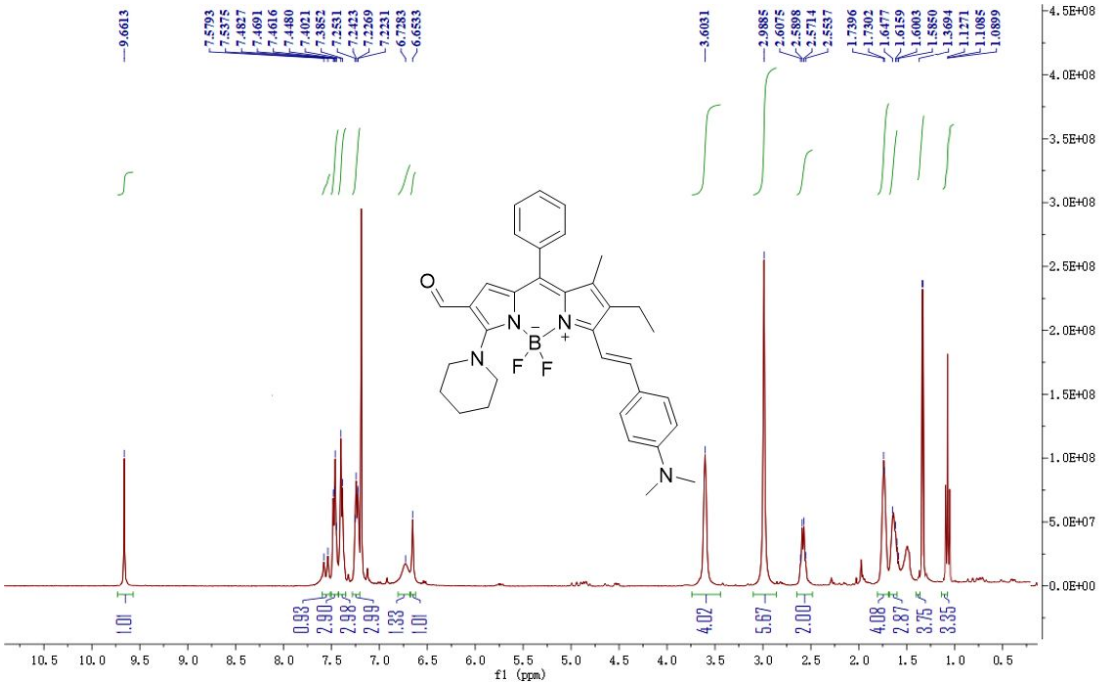

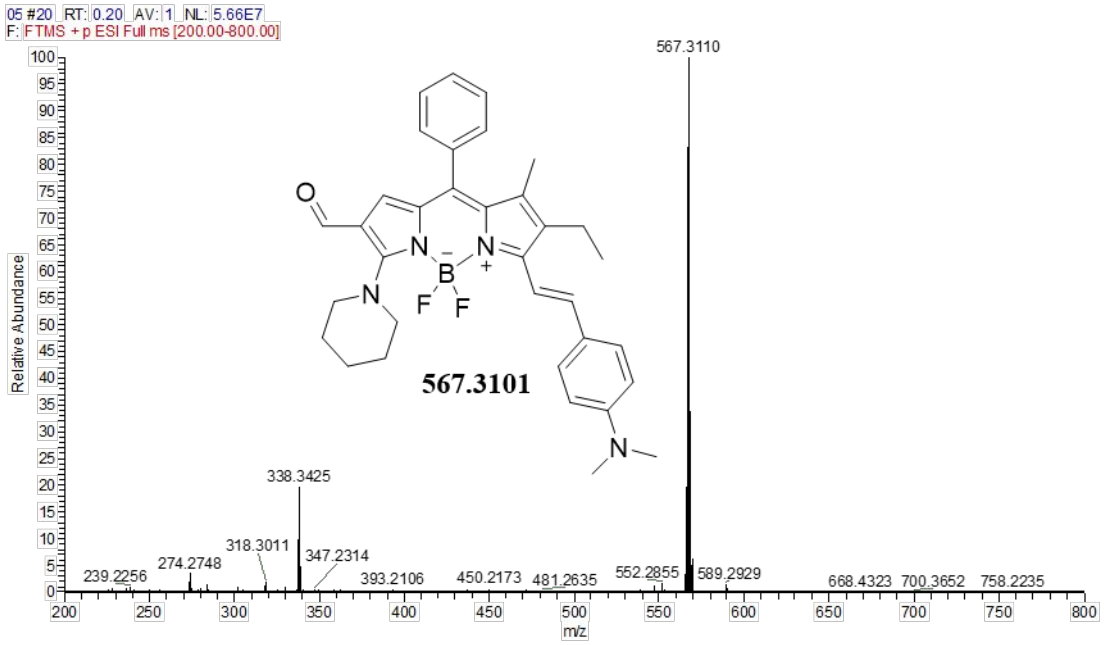

Figure.S20 ^{1}H NMR and ^{13}CNMR of1-ethyl-2-methyl-benz[c,d] indolium salt

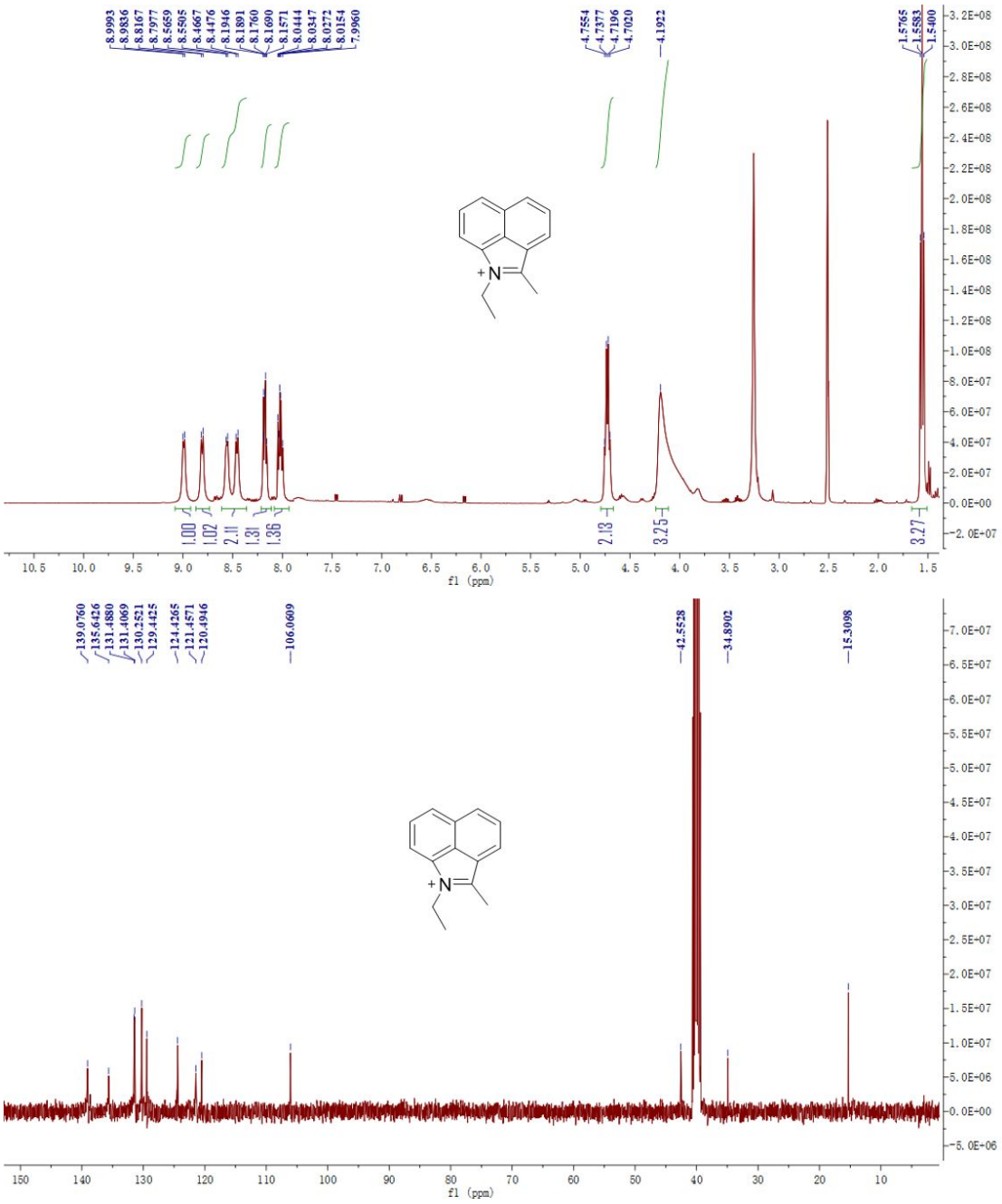

Figure.S21 ^{1}H NMR and HRMS of WD-CH_3

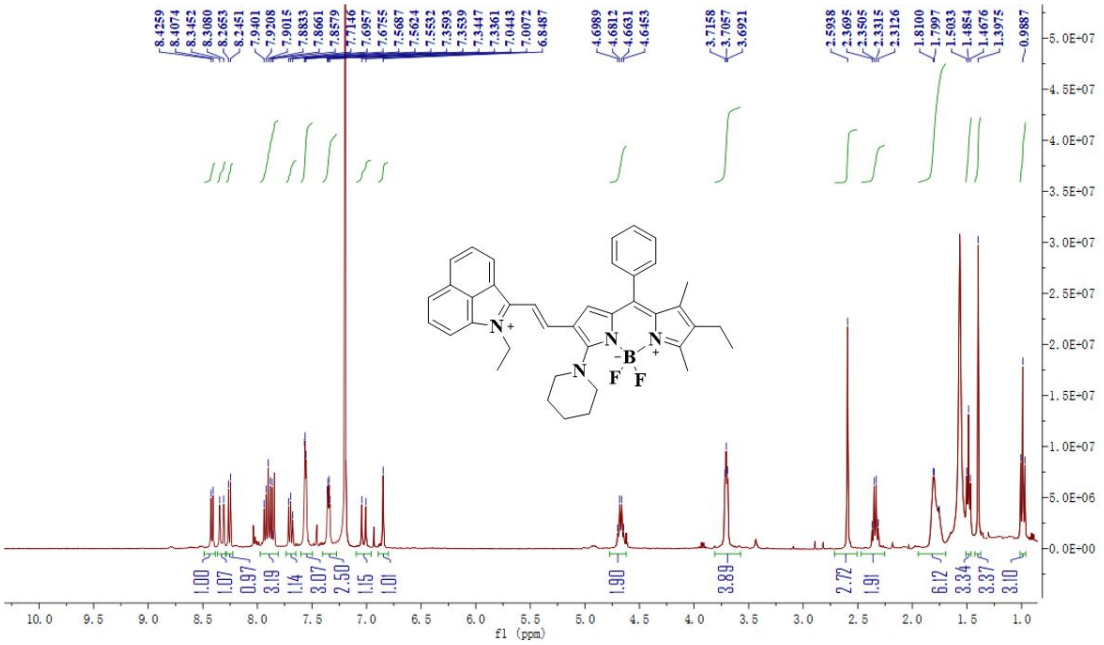

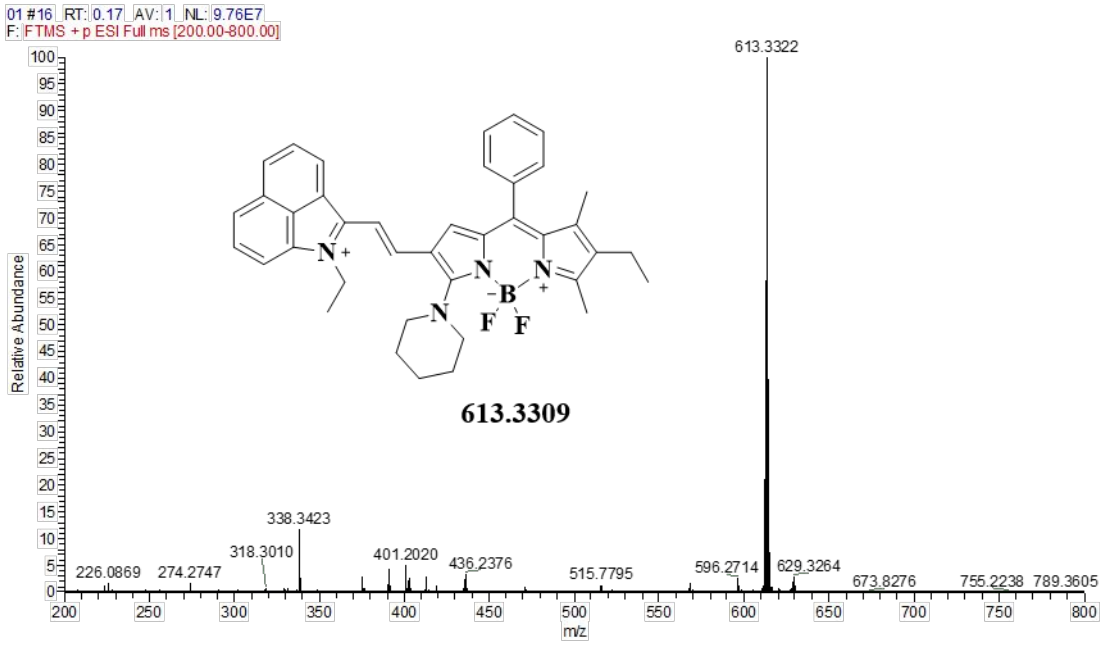

Figure.S22 ^{1}H NMR and HRMS of WD-OCH$_3$

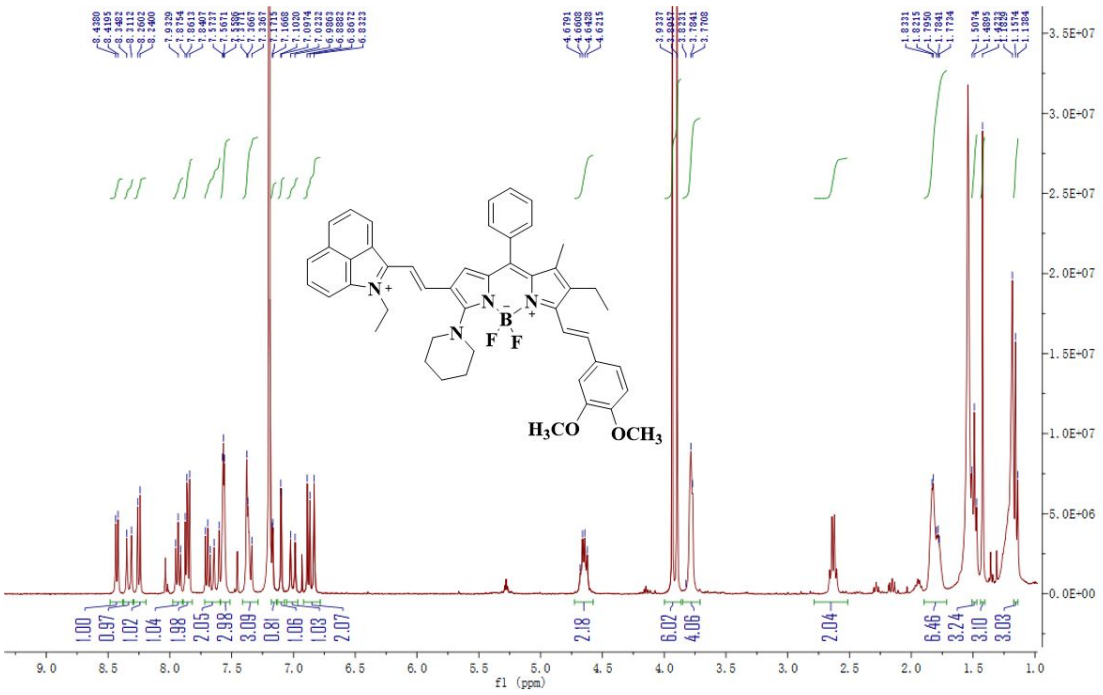

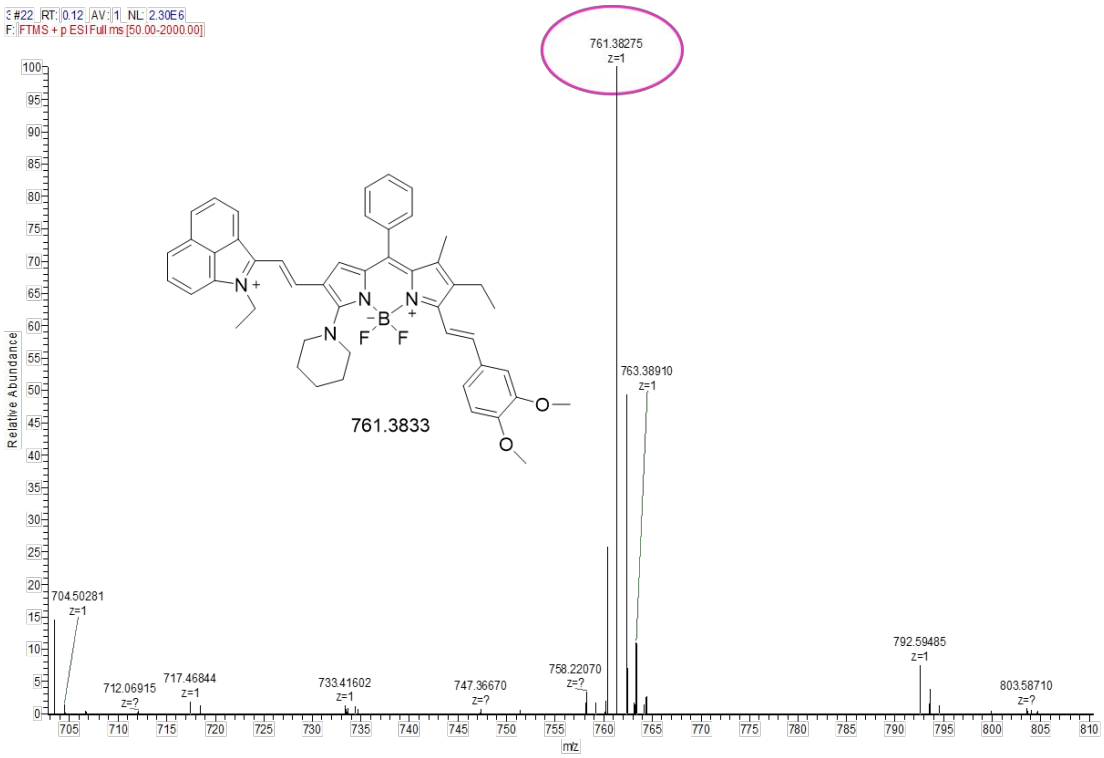

Figure.S23 ^{1}H NMR and HRMS of WD-NME$_2$

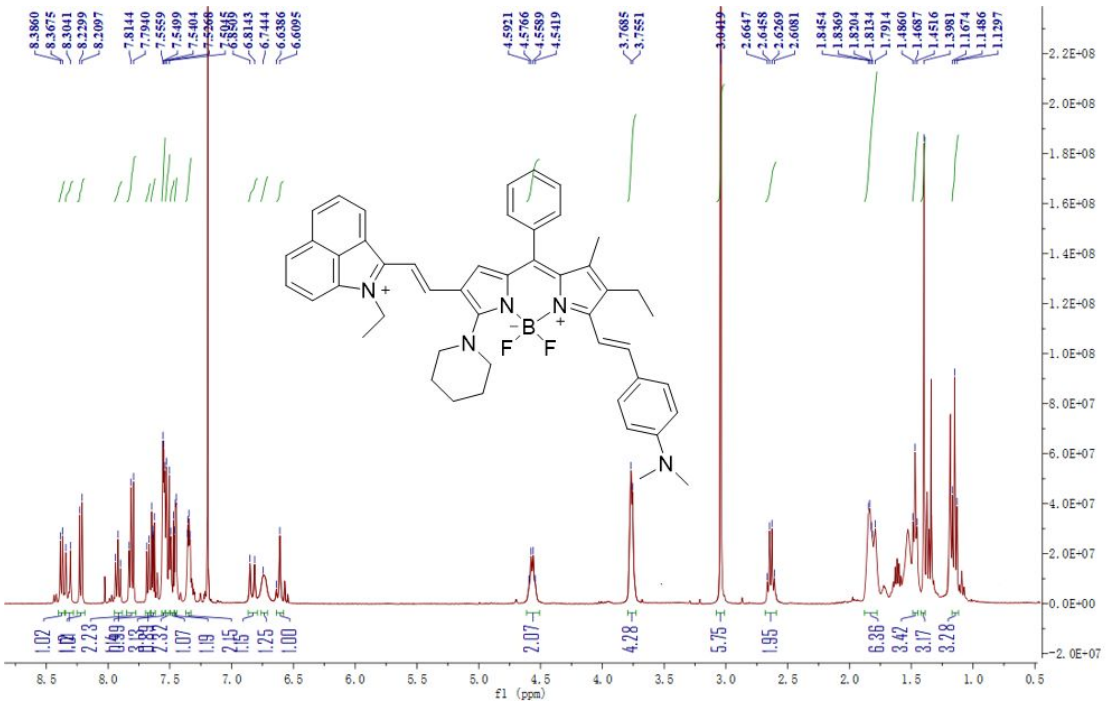

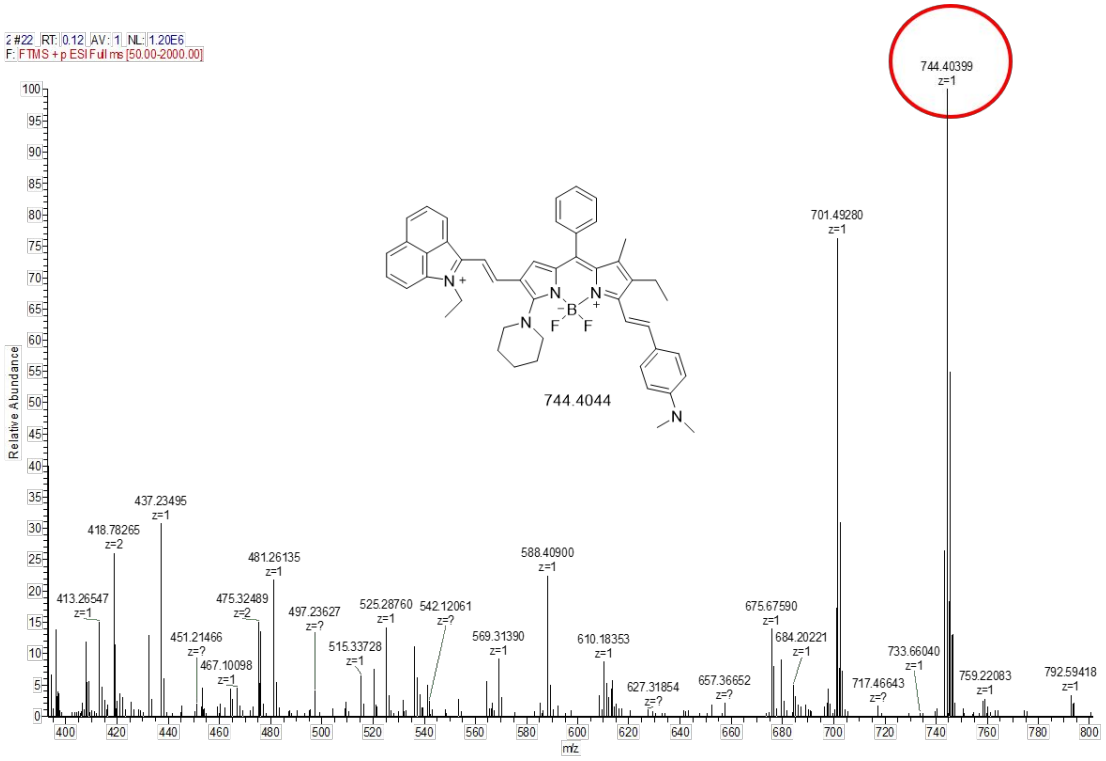

Figure.S24 ^{1}H NMR, ^{13}C NMR and HRMS of WD-NO_2

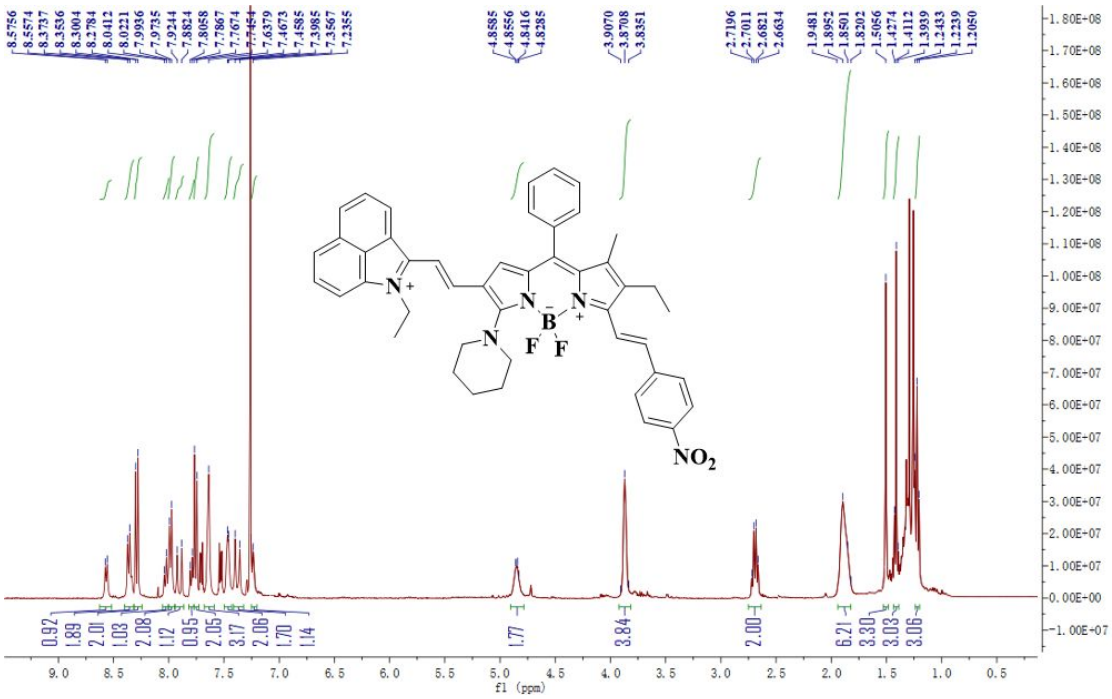

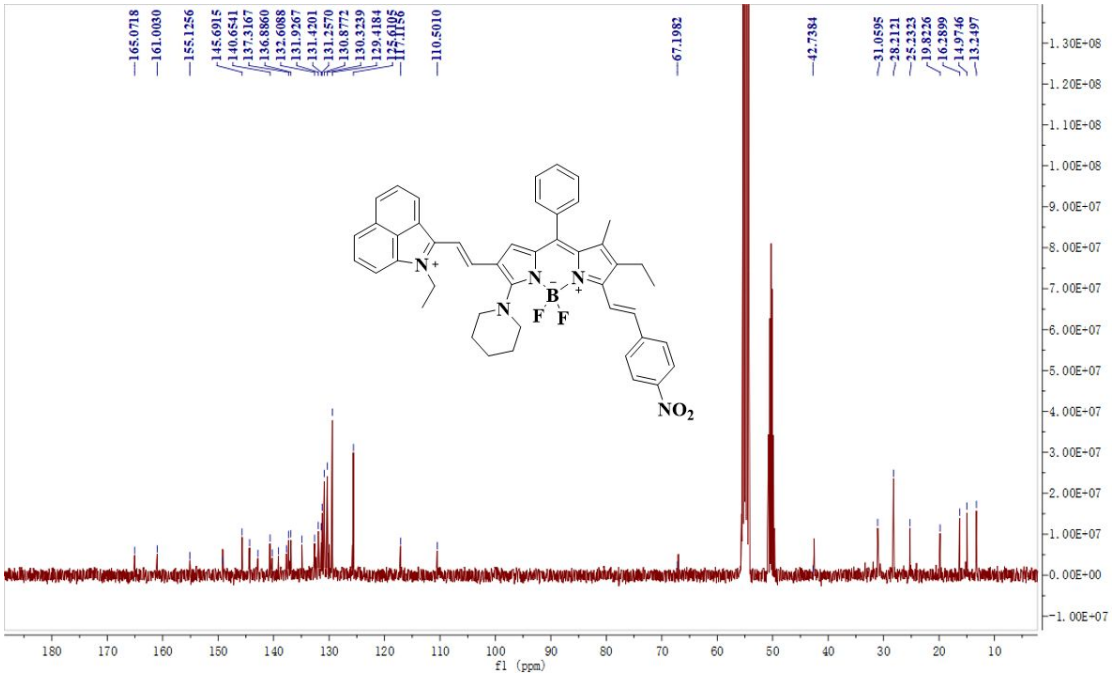

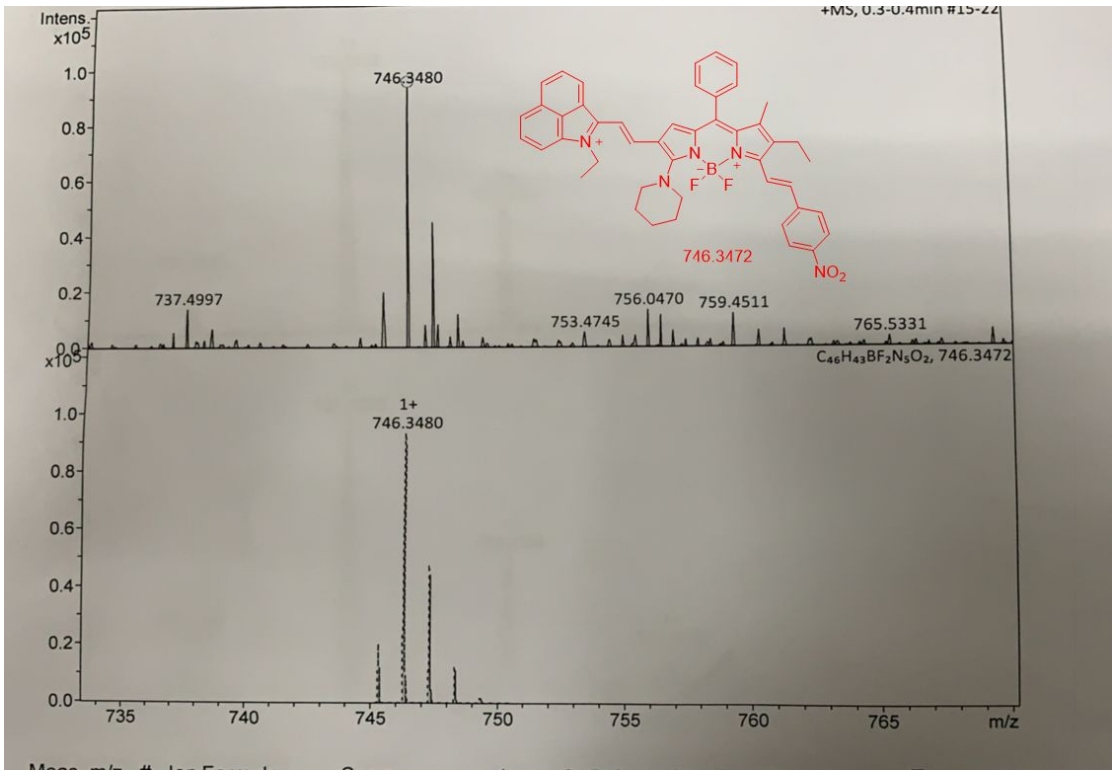

Table S6 Viscosity of the various glycerol/ethanol (v/v) mixtures

Glycerol/ Ethanol (v : v)	η(cp)
0:10	1.52
1:9	3.53
2:8	11.7
3:7	16.3
4:6	25.6
5:5	92.1
6:4	149
7:3	331
8:2	621
9:1	798
19：1	925

Reference

(1) (a) Tao, Z.; Hong, G.; Shinji, C.; Chen, C.; Diao, S.; Antaris, A. L.; Zhang, B.; Zou, Y.; Dai, H. *Angew. Chem. Int. Ed.* **2013**, *52*, 13002; (b) Hu, X.; Tang, Y.; Hu, Y.; Lu, F.; Lu, X.; Wang, Y.; Li, J.; Li, Y.; Ji, Y.; Wang, W.; Ye, D.; Fan, Q.; Huang, W. *Theranostics* **2019**, *9*, 4168.

(2) Ning, P.; Dong, P.; Geng, Q.; Bai, L.; Ding, Y.; Tian, X.; Shao, R.; Li, L.; Meng, X. *J. Mater. Chem. B.* **2017**, *5*, 2743.

(3) Zou, Z.; Yan, Q.; Ai, S.; Qi, P.; Yang, H.; Zhang, Y.; Qing, Z.; Zhang, L.; Feng, F.; Yang, R. *Anal.*

Chem. **2019**. *91,*8574.

(4) Chen, B.; Li, C.; Zhang, J.; Kan, J.; Jiang, T.; Zhou, J.; Ma, H. *Chem. Commun.* **2019**, *55*, 7410.

(5) Zhang, Y.; Li, Z.; Hu, W.; Liu, Z. *Anal. Chem.* **2019**, *91*, 10302.

(6) Guo, R.; Yin, J.; Ma, Y.; Li, G.; Wang, Q.; Lin, W. *Sensors. Actuat. B- Chem.* **2018**, *271*, 321.